frontiers | Frontiers in Marine Science

TYPE Original Research
PUBLISHED 03 August 2023
DOI 10.3389/fmars.2023.1202362

OPEN ACCESS

EDITED BY
El-Sayed Salama,
Lanzhou University, China

REVIEWED BY
Meivelu Moovendhan,
Sathyabama Institute of Science and Technology, India
Tonmoy Ghosh,
Indian Institute of Technology Indore, India
Ghadir El-Chaghaby,
Agricultural Research Center, Egypt

*CORRESPONDENCE
Mohamed Ashour
microalgae_egypt@yahoo.com

RECEIVED 08 April 2023
ACCEPTED 09 June 2023
PUBLISHED 03 August 2023

CITATION
Al-Saeedi SI, Ashour M and Alprol AE (2023) Adsorption of toxic dye using red seaweeds from synthetic aqueous solution and its application to industrial wastewater effluents.
Front. Mar. Sci. 10:1202362.
doi: 10.3389/fmars.2023.1202362

Adsorption of toxic dye using red seaweeds from synthetic aqueous solution and its application to industrial wastewater effluents

Sameerah I. Al-Saeedi[1], Mohamed Ashour[2]* and Ahmed E. Alprol[2]

[1]Department of Chemistry, College of Science, Princess Nourah bint Abdulrahman University, Riyadh, Saudi Arabia, [2]National Institute of Oceanography and Fisheries (NIOF), Cairo, Egypt

This study investigated the potential application of dried powder from red seaweed *Pterocladia capillacea* as an eco-friendly adsorbent for removing Crystal Violet Dye (CV dye) from a synthetic solution. The adsorption conditions for the adsorbent were determined, in batch conditions, by changing different experimental parameters such as initial CV dye concentrations (5, 10, 20, 30, and 40 mg L^{-1}), contact time (15, 30, 60, 120, and 180 min.), adsorbent doses (0.025, 0.05, 0.1, 0.2, and 0.3 g), temperature (25, 35, 45, and 55°C), and pH (3, 5, 7, 9, and 11). The adsorption mechanisms of CV dye onto the *P. capillacea* biomass were examined using various analytical techniques such as FTIR, BET, UV–Visible, and SEM. These characterizations suggest the average BET surface area of *P. capillacea* was 87.17 m^2 g^{-1} and a pore volume of 0.10368 cc g^{-1}. Moreover, according to the FTIR study, the dye has been deposited inside the adsorbent's pores after adsorption. The adsorption behavior of the adsorbent was investigated by performing both kinetic and equilibrium isothermal studies in batch conditions at 25°C. Also, the thermodynamic factors showed the exothermic nature and physisorption of the adsorption process, which tends to be spontaneous at lower temperatures. In addition, Langmuir, Dubinin-Radushkevich, Freundlich, and Tempkin isotherm models were selected to evaluate the adsorption of CV dye on *P. capillacea*. The equilibrium adsorption data were best represented by the Freundlich, indicating multilayer adsorption on the heterogeneous surface. The q_e experiment and calculation values for the Pseudo-Second-Order and interparticle diffusion kinetic models were determined. The results showed that, under optimum conditions *P. capillacea* exhibited 98% removal of CV dye from synthetic wastewater. Moreover, it will help to regenerate the adsorbents that can be reused to adsorb CV dye ions and develop a successful adsorption process. Finally, this study concluded that the dried powdered form of *P. capillacea* is an attractive source for adsorbing CV dye from aqueous solution.

KEYWORDS

***Pterocladia capillacea*, crystal violet dye, bio-adsorbent, adsorption, isotherms**

1 Introduction

The lack of clean water around the world is worsened by pollution caused by the release of untreated industrial effluents (Akin et al., 2022; Isik et al., 2022). The issue is exacerbated by the growth of economies due to uncontrolled population growth and the use of outdated techniques and equipment that require large volumes of water in industrial and agricultural processes (Bhatnagar et al., 2005). To produce completed goods, some industrial processes contain hazardous chemicals, some of which leak into the environment as industrial waste wash (Aksu, 2005). Thus, the difficult issue of creating affordable and effective methods for the treatment of various human activities challenges environmental researchers worldwide (Lee et al., 1999). The discharge of industrial effluents containing hazardous contaminants, such as phenolics, toxic metals, and dyes, even at low concentrations, harms the environment (Khattri and Singh, 2000). Among the most significant categories of pollutants are dyes, which, once they enter water bodies, are harmful to the environment and no longer serve any useful purpose (Dawood, 2013).

Numerous industries, including those in the textile, carpet, food pulp, leather, printing, plastics, cosmetics, and paper sectors, require dyes to color their products. As a result, the wastewater from these industries, which contains dyes, is discharged into water bodies, contaminating them (Ergene et al., 2009). Dyes are generally categorized into cationic, anionic, and non-ionic dyes. The world produces more than 7×10^5 tones and 10,000 different types of dyes every year (Machado et al., 2014). Discharging dyes into the hydrosphere usually produces water of an undesirable color and reduces sunlight penetration in addition to photosynthesis (Banat et al., 1996).

Furthermore, crystal violet dye, also known as gentian violet or methyl violet 10B, was chosen as the study's adsorbate. CV dye can be used as a biological stain, an antiseptic, an antimycotic, an antibiotic, and other things in addition to being utilized as a synthetic dye in the food and textile sectors (Balabanova et al., 2004). CV dye is one of the most commonly used in the textile industry to dye silk and cotton (Sulyman, 2014). Despite its many benefits, CV dye has some risks, including the fact that it may be a clastogen, that digesting it may result in headache and dizziness, and that it has been demonstrated to lower white blood cell count (Docampo and Moreno, 1990). Additionally, studies using mice confirmed the dye to be carcinogenic (Littlefield et al., 1985). Moreover, CV dye in water bodies can have serious toxic effects on humans, such as skin irritation, nausea, itching, gastrointestinal discomfort, chest pain, methemoglobinemia, difficulty breathing, diarrhea, profuse sweating, vomiting, cyanosis, severe headaches (Miller and Miller, 1953; Akin et al., 2022; Erdogan et al., 2022).

Therefore, effluents contain organic dyes which need treatment before being discharged into the environment (Lorenc-Grabowska and Gryglewicz, 2007; Alprol, 2019; Abualnaja et al., 2021; Mansour et al., 2022d). Currently, numerous chemical and physical treatment approaches, including electrochemical treatment, adsorption, oxidation, chemical precipitation and flocculation, reduction, electrolysis, and ion-pair extraction, have been investigated for the removal of various types of contaminants from water (Ng et al., 2002; Sharma et al., 2014; Abate et al., 2020). These approaches are appealing due to their efficiency, but they are sophisticated and costly (Al-Garni et al., 2013). Biological procedures have gained popularity as a viable option because of their low cost, efficacy, capacity to create less sludge, and environmental safety (Chen et al., 2003; Celekli et al., 2010; Anand and Suresh, 2015; Alprol et al., 2019). These mechanisms can convert or degrade this pollutant into water, carbon dioxide, and different inorganic salts (Daneshvar et al., 2007).

The adsorption process is considered one of the most efficient methods for removing synthetic contaminants from aqueous effluents. This process transfers dyes from the aqueous effluent to a solid phase, lowering dye bioavailability to living organisms significantly (Amer and Abdel-Moneim, 2017).

Aquatic plant cells, including microalgae and macroalgae, are regarded as one of the most biologically, ecologically, cost-effective, and efficient applicable materials for bioremediation when compared to terrestrial plants (Alprol et al., 2021a; Mansour et al., 2022c; Mansour et al., 2022e). The diversity and living habitat conditions of aquatic organisms, aquatic plants, or aquatic animals (Mansour et al., 2022c), make them rich sources of biomaterials that may serve in many vital industries such as food supplements, biofertilizers, bioenergy, fine biochemicals (El-Shouny et al., 2015), and effluent water treatments (phytoremediation) (Shao et al., 2019; Alprol et al., 2021b; Ashour et al., 2021; Mansour et al., 2022b). In the phytoremediation process, algal cells form one of the most important factors that affect the efficiency of the phytobioremediation mechanism, in general (Mansour et al., 2022a; Alprol et al., 2023b). The biomass of several algal species has many advantages, such as low cost, high efficiency, regeneration of biosorbents, minimization of chemical and biological sludge, and environmentally friendly adsorbent materials (Ghoneim et al., 2014). The biosorption capacity of algae is attributed to their relatively high surface area and high binding affinity during biosorption (Kusvuran et al., 2011). Nonetheless, adsorption has several disadvantages, including early saturation, a small potential for improving the biological process because cells are not metabolizing, and the absence of any chance for biologically modifying the metal valency state (Ahluwalia and Goyal, 2007). Additionally, using dead biomass requires energy for drying; therefore, the usage of microalgae in batch systems is limited (Brinza et al., 2007).

Among all algae species, red algal species are the most important and economical species in the bioremediation process (Alprol et al., 2023b). *Pterocladia capillacea* is a marine red alga that contains chlorophyll, as well as contains phycoerythrin, an accessory photosynthetic pigment. (El-Sikaily et al., 2011). On rocks close to the coast and in shallow water, they spend their time in the Mediterranean Sea (Aksu, 2005). The various varieties of seaweed may be a more effective and relatively inexpensive dye absorption medium (Alprol et al., 2023a). The marine red alga *P. capillacea* has hollowed, cartilaginous-textured leaves that are typically tiny to moderate in size and multicellular. The phycobioremediation potential of several forms of the red alga *P.*

capillacea for several types of pollutants has been studied and reported in several previous studies. The dried biomass and activated carbon form of *P. capillacea* have the ability to remove several metals from aqueous solutions such as the toxic chromium (Cr^{6+}) (El Nemr et al., 2015) and copper, Cu(II) (El-Sikaily et al., 2011), respectively. El-Din et al. (2016) conducted a study on the potential of phycobioremediation using the biomass form of *P. capillacea* and *Ulva lactuca*, green seaweed, for the removal of pharmaceutical pollutants including clofibric acid, nonylphenol, bisphenol, chloramphenicol, and acetylsalicylic acid from aqueous solutions. The study found that *P. capillacea* had a higher capacity for the bioremoval of all five pharmaceuticals compared to *U. lactuca*. Another study conducted by El-Agawany et al. (2023) aimed to investigate the potential of phycobioremediation using fresh and dried biomass of *P. capillacea* and *Ulva lactuca* for removing four synthetic dyes (RB19, RB5RY2, and RR195) from aqueous solutions. The study concluded that both seaweed species were highly effective in the phycobioremediation of most of the synthetic dyes tested. However, to the best of our knowledge, there are no published data for the adsorption of CV dye on the dried form of red seaweed *P. capillacea*.

This material was chosen for this investigation to test its potential to remove hazardous dyes. Although there is literature on the marine seaweed algae *P. capillacea* as an adsorbent for the removal of heavy metal ions, where previous studies showed the insufficiency of the use of this material in removing toxic dyes from wastewater, this work shows an experimental study on the removal of dyes, particularly CV dye, by using this novel material. Because it significantly improved the adsorption efficacy of the required dyes, it was chosen for the next experiment to fill a gap in the literature. As a result, the current study's main objective is to synthesize powder adsorbent from culture for the removal of CV dye from an aqueous solution that is ecologically friendly, effective, and high in capacity (Alprol et al., 2023a). Furthermore, *P. capillacea* was considered because of its novelty in comparison to agricultural wastes, which may be easily regenerated and recycled, making it suitable for treatment methods. Therefore, the current work was conducted to investigate the effect of the dried red macroalga *P. capillacea* on the removal of CV dye from synthetic contamination. In addition, the kinetics and isotherms of interaction were examined. Also, morphology, surface functionalization, and the pore size of the *P. capillacea* were exposed by scanning electron micrograph (SEM), The Fourier transform infrared spectroscopy (FTIR), UV–vis absorption spectrum (UV), and Brunauer–Emmett–Teller surface area analysis (BET). Moreover, the application to real wastewater of the El-Nobaria drain, Alexandria, Egypt was investigated.

2 Materials and methods

2.1 Biomass materials

P. capillacea samples were collected from the Mediterranean Sea of Alexandria's coasts, Egypt as previously described (Mansour et al., 2022c). Collected samples were washed multiple times with seawater, tap water, and finally distilled water. The clean alga was sun-dried in the air for one week, followed by air oven drying at 70° C for 48 h. The obtained adsorbent was passed through various sieve sizes. The particle fraction is between 0.85 and 1.0 mm. In addition to, approximately 10 g of seaweed powder was mixed with 100 mL of dis. H_2O and subjected to boiling for 30 min under stirring conditions to prepare the algal aqueous extract.

2.2 Dye stock solution preparation

In this work, CV dye was utilized as a model molecule for organic pollutants in general and basic dyes in particular. CV dye has molecular formula $C_{25}H_{30}N_3Cl$ with (a wavelength of 588 nm and a C.I. of 42555), which is known as hexamethyl pararos aniline chloride, in addition to CV dye was purchased from Merck company. The pH of the CV dye solution was adjusted using 0.1 N HCl or 0.1 N NaOH. All of the experiments were carried out with analytical-grade reagents. A stock solution of CV dye (1000 mg L^{-1}) was prepared in distilled water. All working solutions (5–40 mg L^{-1}) were prepared by diluting the stock solution with distilled water at the appropriate amount. The adsorption experiments were carried out at a temperature of 25 ± 2°C.

2.3 Industrial wastewater sampling protocol

A wastewater sample was collected from the El-Naboria drain in Alexandria, Egypt (31° 09′ N and 29° 71′ E), which contains a variety of industrial effluent and agricultural pollutants. The pH was measured using a pH meter (model AD 1080). Turbidity was measured using a LOVIBOND (TB 300 IR) portable turbidimeter. Conductivity was measured with a (Senso Direct 150) probe. Also, total suspended solids (TSS) and total dissolved solids (TDS) were examined through a dry technique at 102–106°C. Because of the low dye concentrations, a small quantity of CV dye was added to produce 5 mg L^{-1} of this dye. The dye solution was filtered to remove precipitates and suspended matter. Samples were collected and stored at 20°C. Laboratory analyses of wastewater were carried out according to the Standard Methods for Examination of Water and Wastewater (Apha, 1926).

2.4 Characterizations

The functional groups of *P. capillacea* were identified by different techniques, including FT-IR (Shimadzu FTIR-8400 S, Kyoto, Japan), UV–Vis spectroscopy (UV-2550, Shimadzu, OSLO, Kyoto, Japan), BET analysis (Micromeritics Instrument Corporation, Model-3Flex, Norcross, GA, USA), and SEM (JSM 6360 LA, JEOL, Tokyo, Japan). The specifications of applied techniques were described previously (Mansour et al., 2022d).

2.5 Batch adsorption experiments

Batch sorption experiments were performed at a constant temperature (25 ± 2°C) on a rotary shaker at 120 rpm using 250 mL capped conical flasks and agitated for the appropriate contact period. CV dye adsorption was investigated using various weights of dried red alga in 100 mL solutions containing 5, 10, 20, 30, and 40 mg L^{-1} of initial CV dye concentration. The concentration of CV dye ions in the solution was measured spectrophotometrically at 588 nm after and before adsorption. All experiments were triplicated, and only the mean values were reported. The following equations (Çelekli et al., 2012; Ahmadi et al., 2020) were used to calculate the quantity of CV dye adsorbed (mg g^{-1}) at a time (t):

$$Removal\,(\%) = [(C_i - C_f) / C_i] \times 100 \quad (1)$$

$$q_e = [(C_i - C_f) \times V] / W \quad (2)$$

where: C_i and C_f are the liquid-phase concentrations of CV dye mg L^{-1} at initial and final concentrations, respectively. While the maximal adsorption at the monolayer (mg g^{-1}) is known as q_e. The volume of the solution is V (L), and the mass of the adsorbent is W (g).

2.6 Isotherm models investigation

To select a suitable model for the design process, equilibrium data should be carefully fitted into various isotherm models as shown in Table 1. Batch adsorption experiments were conducted at room temperature by mixing a solution of 5- 40 mg L^{-1} with 50 mL of CV dye for 3 h at pH 3, and then analyzing the reaction mixture for residual CV dye content.

2.6.1 Langmuir adsorption isotherm

The Langmuir adsorption isotherm assumes that all adsorption sites have a similar affinity for the adsorbate (Langmuir, 1916). The non-linear form of the Langmuir isotherm is described by Equation (3), as presented in Table 1.

2.6.2 Freundlich adsorption isotherm

Freundlich model is an exponential equation that exhibits adsorption on heterogeneous surfaces and it is also used for examining adsorption equilibrium in non-monolayer surfaces (Freundlich, 1906). The Freundlich isotherm model is an empirical relationship describing the adsorption of solutes from a liquid to a solid surface and assumes that different sites with several adsorption energies are involved. The relation between the CV dye

TABLE 1 The equations of the isotherm models.

Model	Equations		Plot
	Eq. No.	Equation	
Langmuir	(3)	$1/q_e=(1/K_aQ_m)\,1/C_e + (1/Qm)$	$1/q_e$ vs. 1/Ce
		Where: C_e is the equilibrium concentration of dye ion (mg L^{-1}), K_a is the Langmuir constant (L mg^{-1}), and Q_m = maximum monolayer coverage capacity (mg g^{-1}).	
Freundlich	(4)	$Log\,q_e = Log\,K_F + (1/n)\,Log\,C_e$	Ln q_e vs. Ln C_e
		Where: the intercept, log K_F, is a measure of adsorbent capacity, the slope 1/n is the adsorption intensity, K_F = Freundlich isotherm constant ((mg g^{-1})(L mg^{-1})1/n), and n = adsorption intensity.	
Tempkin	(5)	$q_e = B\,Ln\,A + B\,Ln\,C_e$	q_e vs. Ln C_e
		Where: A (L g^{-1}) is the Temkin constant and B = (RT)/b while T is the absolute temperature in Kelvin and R is the universal gas constant, 8.314 J mol^{-1} K. The constant b is related to the heat of adsorption.	
Harkins–Jura	(6)	$1/q_e^2 = (B/A) - (1/A)\,Log\,C_e$	$^{1/2}q_e$ vs. Log C_e
		Where: A (g^2 L^{-1}) and B (mg^2 L^{-1}) is two parameters characterizing the adsorption equilibrium.	
Halsey	(7)	$Ln\,q_e = [(1/n)\,Ln\,K] + [(1/n)\,Ln\,C_e]$	Ln q_e vs. Nn C_e
		Where: K (mg L^{-1}) and n are the Halsey isotherm constants.	
Smith	(8)	$q_e = W_{BS} - W_S Ln\,(1 - C_e)$	q_e vs. Ln (1 – C_e)

Where: W_{BS} and W_S are the Smith model parameters.

uptake capacity q_e (mg g^{-1}) of the adsorbent and the residual CV dye concentration C_e (mg L^{-1}) at equilibrium is given by Equation (4).

2.6.3 Temkin adsorption isotherm

The Temkin adsorption isotherm posits that the heat of adsorption reduces with the sorption coverage due to adsorbent–adsorbate interactions (Temkin, 1940). The Temkin isotherm can be simplified to Equation (5) (Table 1).

2.6.4 Harkins–Jura and Halsey models

The HJ model takes into consideration multilayer adsorption, as well as the presence of heterogeneous pore distribution in the adsorbent. The Harkins–Jura adsorption isotherm (Harkins and Jura, 1944) can be expressed in Equation (6). Moreover, the Halsey adsorption isotherm (Halsey, 1952) can be given as described in Equation (7) (Table 1).

2.6.5 Smith model

Smith's model (Smith, 1947) is appropriate for multilayer adsorption. The fitting of Smith equations is particularly visible in heterosporous materials. The Smith model is frequently used in the following form Equation (8) (Table 1).

2.7 Adsorption kinetic investigations

2.7.1 Pseudo-first-order kinetic model

The pseudo-first-order kinetic model (Lagergren, 1898) is expressed as the following Equation (9):

$$Log\,(q_e - q_t) = log\,q_e - k_1 t / 2.303 \quad (9)$$

where: q_t (mg g^{-1}) is the amount of adsorbed CV dye on the adsorbent at time t and k_1 (min^{-1}) is the rate constant of first-order sorption and 2.303 is the constant in the pseudo-first-order equation. A straight line of log ($q_e - q_t$) *vs.* t was obtained with experimental data determined from the intercept and slope of the plot, respectively.

2.7.2 Pseudo-second-order kinetic model

The pseudo-second-order kinetic model as previously described by Ho et al. (Ho and Mckay, 1999) is calculated as the following Equation (10):

$$t/q_t = 1/k_2 q_e^2 + t/q_e \quad (10)$$

where: K_2 (g mg^{-1} min^{-1}) is the rate constant of second-order adsorption. If the Pseudo-Second-Order kinetics were applicable, the plot of t/q_t *vs.* t of the experimental data should provide a straight line, and q_e and K_2 may be deduced from the slope and intercept of the plot, respectively:

2.7.3 Intraparticle-diffusion kinetic model

The intraparticle diffusion equation [82] is explored by Equation (11):

$$q_t = K_{dif} t^{1/2} + C \quad (11)$$

where: K_{dif} (mg g^{-1} $min^{-1/2}$) is the intraparticle diffusion rate constant and C (mg g^{-1}) is related to the thickness of the boundary layer, and K_{dif} and C values are calculated from the slope and intercept of q_t versus $t^{1/2}$ plots, respectively.

2.8 Adsorption thermodynamics investigations

The apparent equilibrium constant (K_d) (L g^{-1}) of the adsorption is defined according to Potgieter et al. (Potgieter et al., 2018), where R is the universal gas constant (8.314 J mol^{-1} K) and T is the absolute temperature in K. The changes in the enthalpy ΔH° and entropy ΔS° parameters should be considered to calculate the Gibbs free energy for adsorption techniques at various temperatures (e.g., 25, 35, 45, and 55°C) using the following (Babarinde et al., 2007; Potgieter et al., 2018; Alardhi et al., 2020) nonlinear Equations (12)–(14):

$$K_d = q_e/C_e \quad (12)$$

$$\Delta G = -RT\,Ln\,K_d \quad (13)$$

$$\Delta G° = \Delta H° - T\Delta S° \quad (14)$$

Ce (mg L^{-1}) is the equilibrium concentration of CV dye. The value uses of ΔH° and ΔS° were calculated from the intercept and slope of the plotted curve of T *vs.* ΔG° of Equation (14) in addition to ΔG°, which can be obtained from Equation (12).

2.9 Reuse of regenerated adsorbents

According to (Dahri et al., 2014), the detailed process of the regeneration experiment was described. Briefly, 0.04 g of adsorbent was treated with 50 mg L^{-1} CV dye, and the suspensions were shaken for 180 min at a temperature of 25°C using an agitation speed of 180 rpm on a shaker that was exposed to 10 mg L^{-1} of CV dye at pH 3 and the amount of CV dye adsorbed was determined. The dye-treated adsorbent was thoroughly washed using distilled water to desorb the dye. The adsorption of red seaweed *P. capillacea* was restored using 0.1 mol L^{-1} of HNO3 as a solvent. The red seaweed *P. capillacea* adsorbent was washed several times with double distilled water as a solvent before being used for the next adsorption cycle, using the same approach as in the adsorption equilibrium studies (Kooh et al., 2016).

3 Results and discussion

3.1 Characterization of adsorbent

3.1.1 SEM

In the current study, SEM analysis was used to examine the surface morphology of the adsorbents before and after CV dye adsorption (Figures 1A, B, respectively). Following CV dye adsorption, the adsorbents' surface shape changes significantly, as does the creation of distinct aggregates on their surfaces. Figure 1 shows an example of SEM images of adsorbents before and after CV dye uptake at ×2000 magnification. *P. capillacea* had a thick and extremely porous morphology with diverse sizes and forms of surface texture (Figure 1A). *P. capillacea*'s interaction with CV dye led to the production of flake-like deposits on its surface, causing the surface to become irregular. Meanwhile, the porous texture of the surface texture vanished, owing to dye adsorption. After coming into contact with CV dye, swelling-like deposits developed.

3.1.2 FTIR

The Fourier transform infrared spectroscopy (FTIR) is useful for identifying functional groups that are capable of adsorbing CV dye ions (Mansour et al., 2022d). Carbons of *P. capillacea* adsorbent were measured using FTIR spectroscopy within the range of 500–4000 cm^{-1} wave number, as shown in Supplementary Figure 1; Table 1. The bands observed at 3289, 2441, and 3729 cm^{-1} in dried red alga represent the bonded–OH group on their surface (Yeamin et al., 2021). The Aliphatic C–H group is represented by the peak at 2854 and 2922 cm^{-1}. The band at 2129 and 2525 cm^{-1} represents C≡C and thiol S–H stretch, respectively. These peaks disappeared after adsorption. Meanwhile, the two bands created after adsorption at 1576 and 1541 cm^{-1} could be assigned to C≡C stretch aromatic and N-H bending types of bonds of amide (II). These groups can be conjugated or non-conjugated to aromatic rings (Villaescusa et al., 2004; Padilha et al., 2005). The absorption band at 1418 cm^{-1} split into three peaks at 1462, 1421, and 1322 cm^{-1} indicating the presence of sp^3 C-H bend. A deformation related to C–O bond was observed in the red alga at peaks 1255 and 1257 cm^{-1}. Also, peaks observed at 1117 and 1159 cm^{-1} after the adsorption of red alga indicate the presence of alkoxy C–O. The absorption bands at 1035–1159 cm^{-1} can be attributed to the C–O stretching vibration of cellulose, lignin, and hemicellulose. While, the peak between 850 and 800 cm^{-1} was for out-of-plane bending of =C–H, i.e., δ=C-H. Several bio-molecules, proteins, and extracellular polymers have been shown to have these functional groups, such as carbonyl, carboxyl, amino, and hydroxyl, which are mainly responsible for the sorption of CV dye through chemical bonding (El-Sikaily et al., 2011).

Furthermore, in this study, we can see the convergence of functional groups, which could be owing to the mechanism of the physical adsorption process related to the Van der Waals forces, and thus the functional groups are comparable before and after adsorption. As a result, there will be no major change in the groups as a result of the surface stability caused by adsorption. Furthermore, functional groups such as carboxyl, carbonyl, hydroxyl, amino have been found within a variety of biomolecules, proteins, and polysaccharides. Because the various functional groups have a high affinity for CV dye, they can form complexes with CV dye ions. According to FTIR analysis, the generation of new absorption bands, changes in absorption strength, and shifts in wave number of functional groups might be caused by dye ion interaction with active sites of adsorbents. The electrostatic affinity between these groups and the cationic dye molecule (CV^+) may cause CV dye sorption on *P. capillacea* adsorbent.

3.1.3 UV

The UV-visible absorption study is one of the most prominent and easy methods to discover the adsorbent process (Kokabi et al., 2017). Owing to the sharpness of the peaks, the UV-VIS spectrum profile of *P. capillacea* biomass extract (Supplementary Figure 2) was chosen between 200 and 800 nm (Mansour et al., 2022d). The compounds were separated at 467.5, 425.5, 297, 269.5, 260, and 207 nm in the profile. The presence of phenolic and alkaloid chemicals in the marine algal is revealed by the peak occurrence at 234–676 nm (Rajeswari and Jeyaprakash, 2019). The existence of phenolic and alkaloid chemicals in *P. capillacea* is indicated by the peak appearance at 234–676 nm (Rajeswari and Jeyaprakash, 2019). In

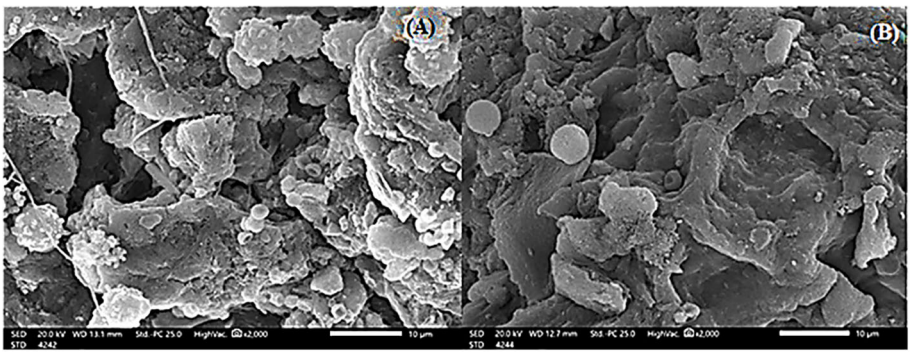

FIGURE 1
SEM of *P. capillacea* before **(A)** and after **(B)** adsorption process.

addition, the extract possesses some comparable alkaloids and glycoside chemicals described based on a comparison of the spectra of seeds and flowers (Sahu and Saxena, 2013; Rajeswari and Jeyaprakash, 2019).

3.1.4 BET

To investigate any changes in the porosity of the sample under investigation, the specific surface area and pore volumes of the adsorbent were investigated. Supplementary Figure 3; Supplementary Table 2 show the nitrogen adsorption-desorption isotherms of impregnated *P. capillacea* at 77.33 K. The textural properties of *P. capillacea* were obtained using the instrument (NLDFT Ads. model) analytical software and certain parameters were obtained using BET, t-plot, and BJH-Des techniques. The average BET surface area (87.1721 $m^2\ g^{-1}$), average particle radius of 1.564 nm, and total pore volume of 0.10368 $Cm^3\ g^{-1}$ were obtained. The desorption branch of the BJH method revealed that the adsorbent contains micropores (1.62 nm) with a pore volume of 0.089 $Cm^3\ g^{-1}$ based on the pore radius distribution of *P. capillacea*. This implies a variety of pore designs in the adsorbent, ranging from micropores to mesopores to macropores that are helpful for phenomena such as the adsorption process and the availability of much more surface area for adsorption (Singh et al., 2022).

3.2 Adsorption studies

3.2.1 Effect of pH

The pH level of the solution is commonly regarded to be one of the primary parameters determining the system's sorption effectiveness (Mansour et al., 2022d). The pH of the adsorbate solution directly influences the dye removal ability of adsorbate. It affects the stability and color intensity of the adsorbate solution. For crystal violet, the color change occurs around pH 0 to 1 for the yellowish-green color, and around pH 11 to 12 for the bluish-purple color. Therefore pH is a significant controlling feature in the adsorption process. In the current work, five pH degrees were carried out (3, 5, 7, 9, and 11) to investigate the influence of solution pH on the effective removal of CV dye by adsorption onto *P. capillacea* (Figure 2). The present work showed that when the pH of the solution was decreased, the efficiency of CV dye removal percentages increased. It has been found that by increasing the initial pH 3 to 11, the percentage removal of CV dye treatment decreases. The high percentage efficiency of CV dye removal in an acidic medium reached a high adsorption percentage of 94.5% at pH 3, and then, the uptake declined with a further increase in pH for the synthetic solution. This may be attributed to the electrostatic interactions between the positively charged adsorbent and the negatively charged dye anions (Bhatti et al., 2021). Both the dye chemistry in water and the cell surface dye binding sites are influenced by the solution pH. In solution, the dye releases colored dye anions (Dawood and Sen, 2014). The complex heteropolysaccharides and lipid components of red algae's cell wall composite produce various functional groups, including carboxyl, hydroxyl, sulfate, and other charged groups (Foo and Hameed, 2011). The biomass will have a net positive charge at lower pH values. At acidic pH, it is expected that nitrogen-containing functional groups, such as amines, will also be protonated, increasing the concentration of H^+ ions and positively charging the biomass's surface (Mansour et al., 2022c). The electrostatic attraction between these negatively charged dye anions and the positively charged cell surface may contribute to higher uptakes that are observed at lower pH values, for which hydrogen ions function as a ligand for bridging between the dye molecule and the algal cell wall. Changes in surface properties and charge can be attributed to the decrease in the dye's ability to adsorb on algae as pH increases (Salleh et al., 2011). The different colors of CV dye are a result of the different charged states of the dye molecule. In the yellow form, all three nitrogen atoms carry a positive charge, of which two are protonated, while the green color corresponds to a form of the dye

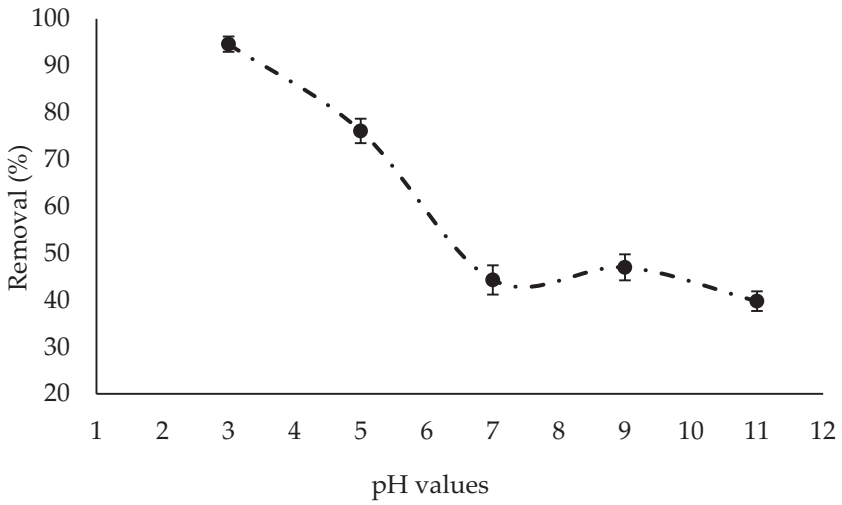

FIGURE 2
The impact of different pH values of P. capillacea on CV dye removal (initial concentration of CV dye 5 mg L^{-1} : temperature 25 ± 2 °C; adsorbent dose 0.05 g; initial volume: 50 mL; contact time: 180 min).

with two of the nitrogen atoms positively charged. At neutral pH, both extra protons are lost to the solution, leaving only one of the nitrogen atoms positively charged. The pKa for the loss of the two protons is approximately 1.15 and 1.8 (Mbacké et al., 2016).

3.2.2 Doses of adsorbent biomass

The biomass amount is important because it indicates a material's capacity for a specific initial concentration under operating conditions (Sarı and Tuzen, 2009). The influence of adsorbent dosage on the adsorption process was examined by altering the adsorbent amount of 0.025, 0.05, 0.1, 0.2, and 0.3 g at a temperature of 25 ± 2°C, and pH 3 and adsorbate concentration of 5 mg L^{-1} at various contact times for 180 min. Figure 3 demonstrates that the percentage removal was gradually increased with increasing the adsorbent dosage of *P. capillacea* from 75. 7% to 96.1% at 0.025 to 0.3 g for the synthetic solution. The development in removal efficiency can be ascribed to an increase in the adsorbent's total surface area and active adsorption sites (Lee et al., 2019). If all other parameters stay constant, the adsorption capacity rises marginally with increasing doses of adsorbent at 0.025 to 0.3 g. This trend is to be expected because increasing the adsorbent dose increases the number of adsorbent molecules available, which led to augmented surface area and thus leads to more opportunities for dye ions to adhere to the adsorbent (Cusioli et al., 2020). Therefore, the trend of increasing the removal capacity occurs because more adsorption sites will be provided for the dye ions (Cusioli et al., 2020).

3.2.3 Temperature

Another important factor to consider is the effect of temperature on adsorption, which impacts the adsorbent's adsorption capacity (Abate et al., 2020). To investigate the effect of temperature on the adsorption of the adsorbent biomass *P. capillacea*, four different temperature levels (25, 35, 45, and 55°C) were utilized with a CV dye level of 5 mg L^{-1} (Figure 4). The increase in temperature gradually improves the adsorption removal capacities of adsorptive pollutants such as dyes, due to increased surface activity and kinetic energy of the adsorbate, while it may damage the physical structure of the adsorbent (Abdi and Kazemi, 2015). In the current study, the results show that the adsorption efficiency varies in the selected temperature range, and dye adsorption efficiency decreases as temperature increases. The higher removal percentage was shown at 25°C with 78.9% for synthetic wastewater. As a result, it indicated that the adsorption process was exothermic due to the equilibrium uptake of CV dye reduced with increasing temperature, in addition to the mechanism being mostly physical sorption, governing at lower temperatures. At high temperatures, the weakening of interactions between dye ions molecules and *P. capillacea* of adsorbents may result in a reduction in red algae adsorption (Meena et al., 2005; Cheraghi et al., 2016). Adsorption is always exothermic due to the adsorption leads to a reduction in the residual forces on the outside of the adsorbent. Adsorption is an exothermic process since surface particles of the adsorbent are unstable and when the adsorbate is adsorbed on the surface, the energy of the adsorbent decreases, and this results in the

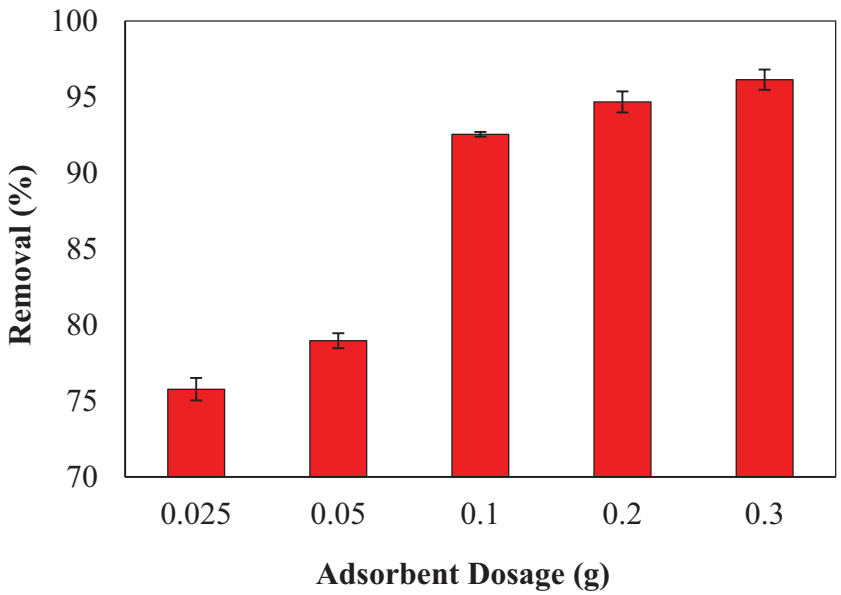

FIGURE 3
The impact of different initial doses (g) of P. capillacea on CV dye removal (%) (initial concentration of CV dye 5 mg L^{-1}: temperature 25 ± 2°C; pH: 3; initial volume: 50 mL; contact time: 180 min).

10.3389/fmars.2023.1202362

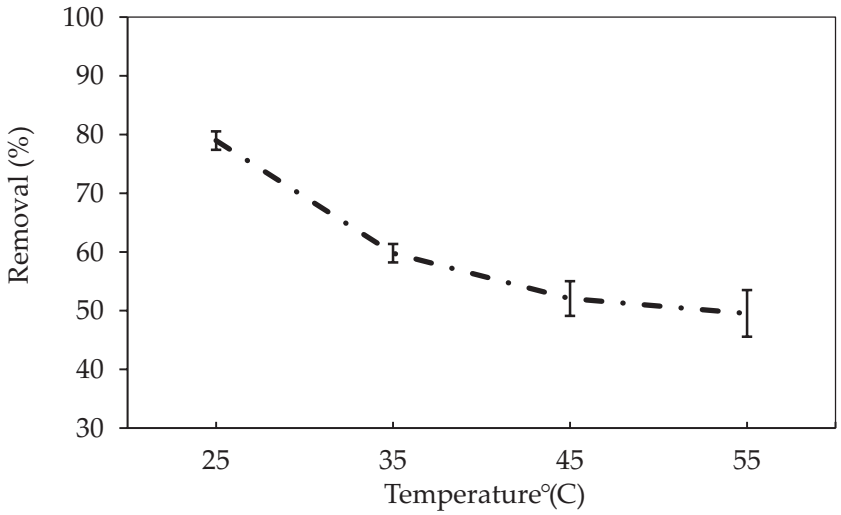

FIGURE 4
The impact of temperatures (°C) of *P. capillacea* on CV dye removal (initial 38 concentration of CV dye 5 mg L^{-1}: concentration of 5 mg L^{-1}; at pH: 3; initial volume: 50 39 mL; contact time: 180 min).

evolution of heat. Therefore, adsorption is always exothermic. Moreover, higher temperature can deactivate active sites resulting in reduced dye adsorption (Tahir et al., 2016).

3.3 Kinetic study

3.3.1 Effect of initial contact time

The equilibrium adsorption of *P. capillacea* was studied at several contact time intervals to examine the effect of various contact times on adsorption. As presented in Figure 5, contact times ranging between 15 and 180 min on the removal of CV dye have been carried out with an initial dye concentration of 5 mg L^{-1} at pH 3. When the maximum CV dye adsorption onto *P. capillacea* was obtained, the equilibrium was determined to be about 30 min. The adsorption of CV dye was increased as the quantity of *P. capillacea* and contact duration increased. It was found that the rate of removal is extremely rapid in the first 15 min, with percentage removal of approximately 73% and 75% for both synthetic solution and effluent wastewater, respectively, and gradually increasing up to the equilibrium rate of adsorption, for which the results indicate that the adsorption removal of CV dye increased from 73 to 86.9% in the range of 15–30 min and then decreased from 85–82% in the range of 60–180 min for the synthetic solution. This was most probably caused by the processes of adsorption and desorption that follow the saturation of adsorbent surfaces with CV dye (Azizi et al., 2017). The availability of the positively charged surface of *P. capillacea* resulted in the fast electrostatic attraction of the anionic

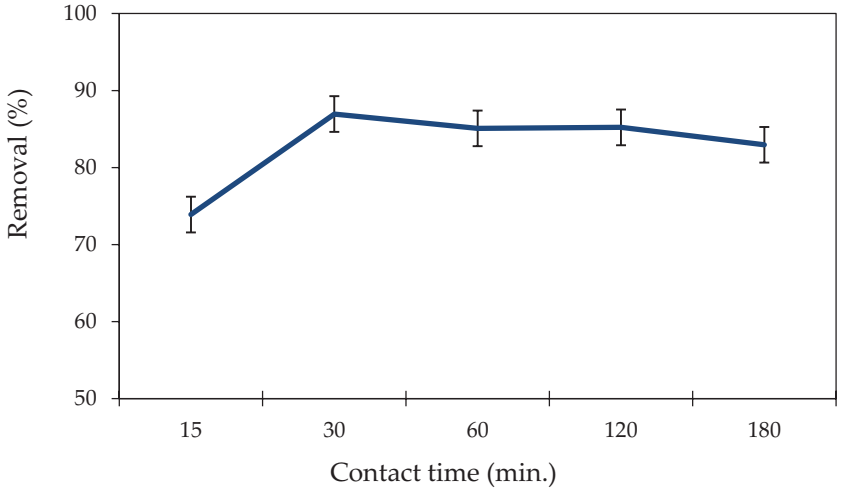

FIGURE 5
The impact of different contact times (min.) of P. capillacea on CV dye removal (initial concentration of CV dye 5 mg L^{-1}: 25 ± 2°C; pH: 3; initial volume: 50 mL; adsorbent dosage 0.05 g).

CV dye from the solution, explaining the rapid adsorption at the initial contact time. Also, the change in adsorption rate might be attributed to the fact that all sites are initially occupied and the gradient in solute concentration is very high (Ghaedi et al., 2012). As a result, the reduced adsorption rate is caused by a decrease in the number of vacant sites and lower dye concentrations. The low adsorption rate, particularly near the end of the examinations, suggests that a monolayer of CV dye might form on the adsorbing surface (Pathania et al., 2017). This might be owing to a shortage of available active sites for further dye adsorption after achieving equilibrium (Liang et al., 2010).

3.3.2 Kinetic models

To assess the potential adsorptive mechanism of pollutants, many kinetic models have been presented. The mechanism of adsorption is determined by the sorbent's physical and/or chemical properties, as well as the mass transport process. Three models (Pseudo-first-order kinetic (Supplementary Information), Pseudo-second-order kinetic, and Intraparticle diffusion model were utilized to examine the mechanism of CV dye adsorption (Figures 6A–C, respectively).

3.3.2.1 Peudo-second-order kinetic model

Plotting t/q_t versus t for the adsorption of CV dye by dried red alga was investigated and given a straight line, and the second-order rate constant (k_2) and q_e values were determined (Table 2; Figure 6B). The pseudo-second-order kinetic model was used to describe the adsorption of CV dye from synthetic wastewater by red algae with ($R^2 > 0.952$). The values of q_e estimated using the PSO model (1.08 mg g^{-1} for the synthetic solution) agreed with the values of q_e, exp (1.190 mg g^{-1} for the synthetic solution). This implies that the CV dye adsorption system follows the pseudo-second-order kinetic model throughout the adsorption period and reveals that the adsorption process conforms to a pseudo-second-order model, as well as that it appears to be chemically controlled (Figure 6B).

3.3.2.2 Intraparticle-diffusion model

Due to the low adsorbate concentration that is already in the solution, the intraparticle diffusion model is divided into three phases: the fast external surface adsorption phase, the intraparticle diffusion phase, and the slow equilibrium phase (Kooh et al., 2016). The overall adsorption rate in a porous adsorbent must consider the three steps of external mass transfer, intraparticle diffusion (Figure 6C), and adsorption on an active site inside the pores. The following mathematical equation is used to characterize the therapy of CV dye using the intraparticle diffusion model (type 2) (Weber and Morris, 1963). Where C is the intercept and ki is the intraparticle diffusion rate constant (mg g^{-1} $min^{1/2}$), which can be evaluated from the slope of the linear plot of q_t versus $t^{1/2}$ as presented in Figure 6C. This investigation demonstrates that straight lines did not pass through the origin, and the R^2 value was 0.383. The curve did not pass through the origin indicating that intraparticle diffusion was not the sole rate-determining step and that boundary layer diffusion controlled the adsorption to some (Cheung et al., 2007). The deviation of the diagram from the path may be due to the rate-limiting step dictated by boundary layer diffusion (El-Said et al., 2018). Nevertheless, the k_{dif} value was 0.096 mg g^{-1} $min^{1/2}$. The external surface adsorption may have happened quickly within the first 15 min of agitation. No region had a C value equal to zero, as seen in (Supplementary Table 3; Figure 6C), indicating that these lines do not pass through the origins, which indicates that intraparticle diffusion is not the rate-limiting step. Özacar and Şengil (2004) found a similar observation regarding the adsorption of dispersion dye into alunite. In addition, Kooh et al. discovered the elimination of Rhodamine B dye from an aqueous solution by Casuarina equisetifolia needles (Kooh et al., 2016).

3.4 Equilibrium and isotherm adsorption study

3.4.1 Initial CV dye concentrations

The impact of initial dye concentration is determined by the direct relationship between the initial dye concentration and the availability of adsorbing sites on the adsorbent's surface (Mashkoor and Nasar, 2020). CV dye solution concentrations between 5–40 mg L^{-1} were used to study the effect of initial CV dye concentration on the removal percentage of *P. capillacea* (Figure 7). In general, the increase in the initial concentration of the dye enhances the interaction between the dye molecules and the surface of the adsorbent (Lee et al., 2019). Kareem et al. (Kareem et al., 2016) cited that, during the initial adsorption stage, high amounts of vacant surface sites are obtainable for the adsorption process. The adsorption behavior clearly showed a reduction in the percentage of adsorption on *P. capillacea* as the initial concentration increased, and so increased the adsorption capacity. It was observed that the amount of CV dye adsorbed by a unit weight of *P. capillacea* is decreased with increasing CV dye concentration. The percentage of removal of CV dye in the synthetic solution reduced from 91% to 49.9% as the initial concentration of CV dye grew from 10 to 40 mg L^{-1}, while the adsorbent capacity (q_e) increased from 37.4 to 52.6 mg g^{-1} as the initial concentration of CV dye increased from 5 to 40 mg L^{-1}. These results may be explained on the basis that the increase in the number of ions competing for the available binding sites and also because of the lack of active sites on the adsorbent at higher concentrations (Surchi, 2011). Initial dye concentration offers a considerable driving power to overcome all dye mass transfer resistances across the aqueous and solid phases, implying that initial dye concentration influenced both dye decolorization percentages (Nassar et al., 2015).

3.4.2 Isotherm models

Isotherms are a basic and crucial necessity for the study of adsorption systems; moreover, isotherms are employed for design purposes (Abdel Wahab, 2007). In addition, fitting the isotherm data to multiple isotherm models is a critical step in determining a suitable model that may be utilized for design purposes.

10.3389/fmars.2023.1202362

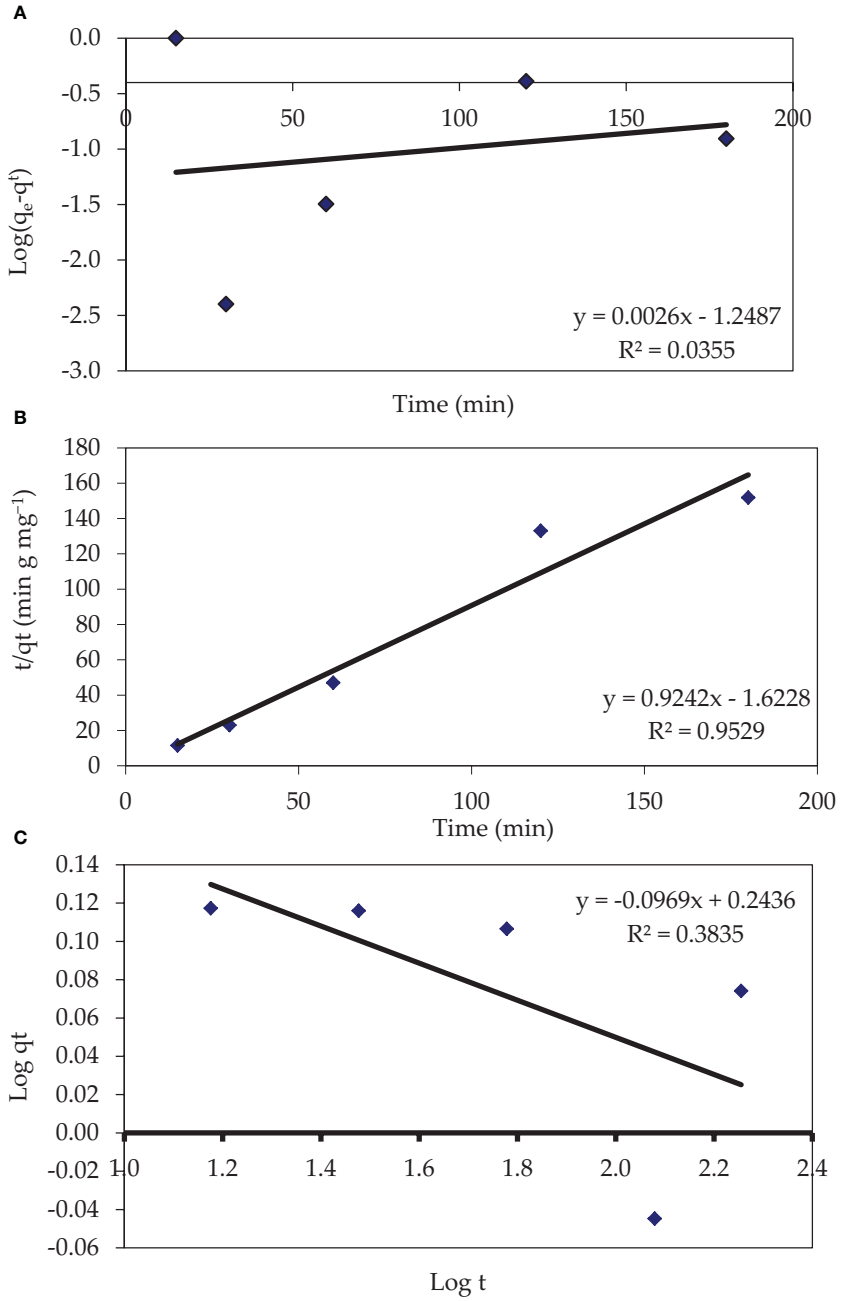

FIGURE 6
Pseudo-second-order-kinetic **(A)**, Pseudo-second-order-kinetic **(B)**, and Interparticle-diffusion-kinetic **(C)** models for the elimination of CV dye onto *P. capillacea* (pH 3 with 0.05 g of adsorbent; 5 mg L^{-1} of dye concentrations at 25 ± 2 °C; initial volume: 50 mL; contact time 10, 20, 30, 60, 120, and 180 min).

TABLE 2 Thermodynamics factors for the sorption of CVD onto *P. capillacea*.

Temperature (°C)	ΔG° (kJ mol^{-1})	ΔH° (kJ mol^{-1})	ΔS° (J mol^{-1})
25	−7.29	−0.1125	25.4
35	−9.91		
45	−11.06		
55	−10.66		

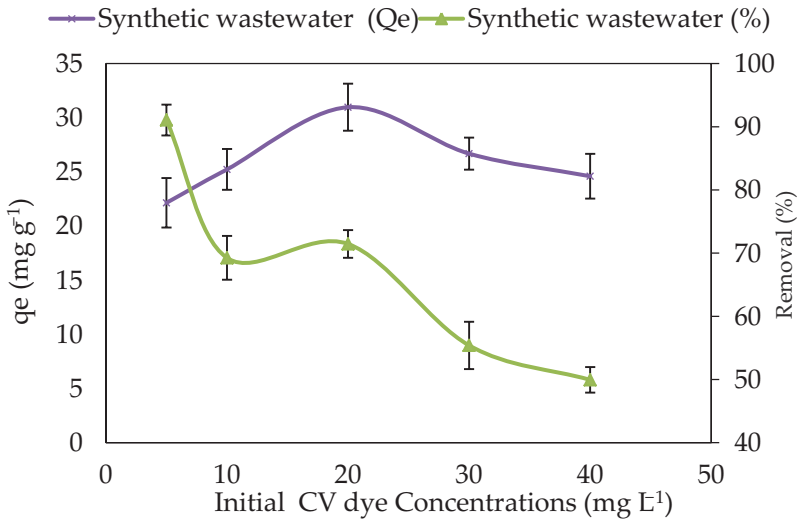

FIGURE 7
The impact of different initial CV dye concentrations on their adsorbent onto P. capillacea (adsorbent amount: 0.05 g; temperature 25 ± 2°C; initial volume: 50 mL; pH: 3; contact time: 180 min).

3.4.3 The Freundlich isotherm

Using the same set of dried red alga experimental data, the applicability of the experimental Freundlich isotherm was investigated based on sorption on heterogeneous surfaces by graphing Log (q_e) *vs.* Log (q_e) (C_e). As demonstrated in Figure 8B, the CV dye sorption isotherm followed the Freundlich model (Freundlich, 1906). For synthetic wastewater, the isotherm data fit the Freundlich model well (R^2 = 0.995). This might be because the adsorbent surface is nonhomogeneous and there could be more than one type of sorption site on the surface (Diquarternasi, 2009). Moreover, the Freundlich model constants K_F and n are determined from the intercept and slope of the plot, respectively (Figure 8). The constant K_F can be defined as the adsorption coefficient which represents the quantity of adsorbed CV dye for a unit equilibrium concentration, while 1/n is a measure of the adsorption intensity or surface heterogeneity. The values of the constants K_F and n were calculated to be 7.19 (mg g^{-1}) and 3.63, respectively, for synthetic wastewater solution. The adsorption intensity or surface heterogeneity is measured by the calculated 1/n factor. Meanwhile, Table 3 demonstrates that 1/n > 1 indicates favorable adsorption, which requires significant interactions between the adsorbate molecules. Therefore, the adsorption manner is reversible and not just limited to monolayer formation. Multilayer dye adsorption onto the adsorbent is possible, with non-uniform heat and affinity distributions across the heterogeneous surface. The Freundlich constant n tends to be in the range of 1 to 10 for favorable adsorption. While 1/n = 1 suggests adsorption leading to similar adsorption energies for all sites, larger values of n indicate stronger interactions between the adsorbed and dye (Foo and Hameed, 2010). The n value in this study was 3.63; consequently, the interaction between the adsorbent and CV dye surface is heterogeneous.

3.4.4 Temkin isotherm

As a result, the Temkin adsorption isotherm model Tempkin isotherm model considered the effects of indirect adsorbate–adsorbate interaction isotherms which explained that the heat of adsorption of all the molecules on the adsorbent surface layer would decrease linearly with coverage due to adsorbate–adsorbate interactions. The Temkin isotherm graphs for the adsorption data are shown in Figure 8. The low correlation coefficients, which are reported in Table 2, suggest that the Temkin isotherm is suitable for the synthetic solution for the adsorption of CV dye by *P. capillacea*.

3.4.5 Harkins–Jura, Halsey, and Smith models

The Harkins–Jura model can be defined as having multilayer adsorption and dispersion of heterogeneous pores, while the Halsey isotherm equations are appropriate for multilayer adsorption. In particular, hetero-porous solids can fit these equations. Table 4 shows the isotherm parameters of the Harkins–Jura and Halsey models (Figures 9A, B, respectively). In this study, the correlation coefficients for the Harkin–Jura and Halsey equations were 0.952 and 0.959, respectively. This may indicate that the Harkins–Jura and Halsey models are applicable. The Smith model applies to hetero-porous solids and multilayer adsorption, as well as helping describe the adsorption isotherm of a biological substance. Table 4 shows the isotherm parameters of all the evaluated isotherm models. The constants of the Smith model can be determined from the linear plot of q_e *vs.* Ln (1 - C_e) as shown in Figure 9C. The adsorption isotherms were effectively described by Smith models. The Smith equations, on the other hand, were less successful in modeling the CV dye isotherms onto *P. capillacea* because the Smith Model had lower R^2 values.

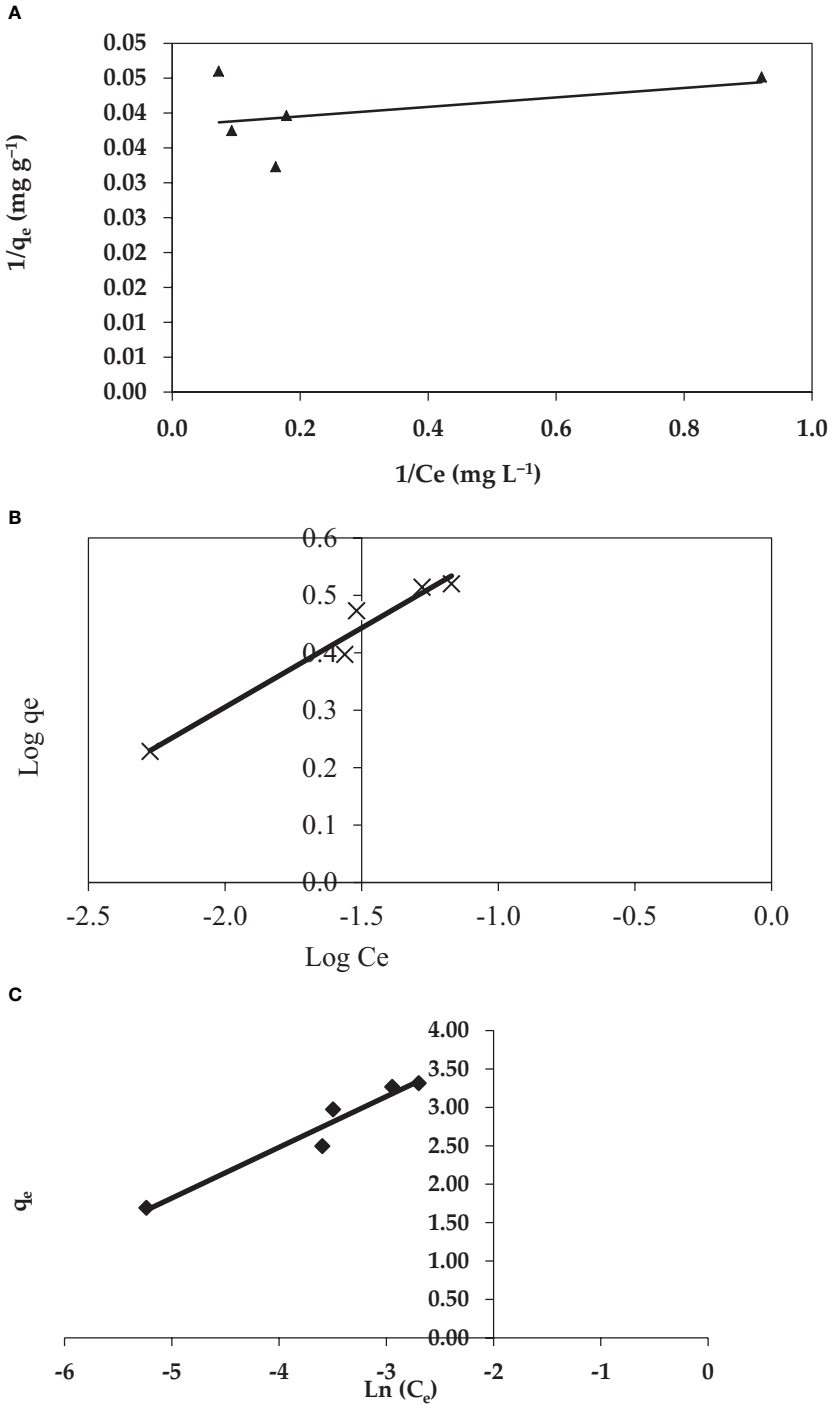

FIGURE 8
The fitting plot of the **(A)** Langmuir, **(B)** Freundlich, and **(C)** Temkin isotherm equations.

3.5 Thermodynamic study

Thermodynamics is used to determine whether a process is chemical or physical, endothermic or exothermic, and spontaneous or non-spontaneous. Batch experiments were conducted at various temperatures to measure the activation energy (Ea), Gibbs free energy (ΔG°), enthalpy (ΔH°), and entropy (ΔS°) of the process. Table 5 shows the calculated thermodynamic parameters for the adsorption system, such as ΔH°, ΔS°, and ΔG°. In general, the range of ΔG° values for physisorption is between −20 and 0 kJ mol^{-1}; however, the chemisorption process is between−80 and−400 kJ mol^{-1}. The activation energy measurements obtained in this investigation show that the CV dye was absorbed into the adsorbent via a physisorption process. Table 2 reveals that the obtained ΔH° values were negative, demonstrating that the adsorption process was exothermic and the mechanism was mainly physical adsorption. This showed that when the

TABLE 3 Correlation coefficients and adsorption isotherm models constants of CV dye onto *P. capillacea*.

Model	Isotherm Parameters	Value
Langmuir	Q_m (mg g^{-1})	5.714
	K_a (L g^{-1})	87.5
	R_L	0.016
	R^2	0.673
Freundlich	n	3.63
	K_F ((mg g^{-1})(L mg^{-1})1/n)	7.19
	1/n	0.524
	R^2	0.959
Tempkin	A_T (L mg^{-1})	2318.50
	b_T (J mol^{-1})	0.68
	R^2	0.945
Halsey isotherm	$1/n_H$	0.2759
	K_H	0.729
	R^2	0.959
Harkins-Jura isotherm	A_{HJ}	4×10^{-3}
	B_{HJ}	0.9
	R^2	0.952
Smith isotherm	W_{bs}	1.816
	W_s	24.79
	R^2	0.841

temperature increases, the adsorption of dye onto the adsorbent decreases. These results were similar to Srinivasan and Viraraghavan (2010) that adsorption onto algae is typically an exothermic process. Moreover, the positive values of ΔS° suggest that the system is becoming more disordered as a result of a potential loss of water that surrounded the CV dye ions during their adsorption to the adsorbent active sites (Yan et al., 2013). Similarly, the negative values of ΔG° suggested that the adsorption was spontaneous, and the increase in the value of ΔG° with increasing temperature indicates that the reaction was less favorable at higher temperatures (Azizi et al., 2017).

3.6 Regeneration study of *P. capillacea*

The regeneration of *P. capillacea* for reuse in CV dye removal was investigated and the adsorption efficiency of each cycle was calculated according to Equation (1) and reported in Figure 10. The number of regeneration cycles increased from one to three. The regeneration result shows that the *P. capillacea* loses only 38% of its adsorbing capacity after three cycles for the synthetic solution. the effectiveness of CV dye adsorption from *P. capillacea* in synthetic solution decreased from 69.59% to 61.97%. The adsorption removal of this absorbent was slightly decreased during the reusability cycles. After 3 cycles the adsorption removal was still more than 61.97% which was probably due to the drop of adsorption sites due to the accumulation of adsorbents (Uyar et al., 2010). Some of the dye molecules may have been trapped deep inside the aggregates of *P. capillacea* particles. Thus, this adsorbent is suitable for toxic dye removal with ease of reusability. Moreover, the red alga *P. capillacea* can be regenerated and maintain high adsorption effectiveness even after being used three times.

TABLE 4 A summary of different adsorbent materials for the removal of CV dye from real wastewater and synthetic solutions.

Adsorbent	Pollutant Type	Optimized Conditions *	q_{max} (mg g^{-1})	References
Natural zeolite	Real wastewater	pH 10, 1 g L^{-1}, 25°C, 24 h, 200 mg L^{-1}	106.67	(Sarabadan et al., 2019)
Lemongrass leaf	synthetic solution	pH 5, 30 g L^{-1}, 25°C, 4 h, 60 mg L^{-1}	36.1	(Putri et al., 2020)
Solid waste of rosewater extraction	Real wastewater	pH 4, 2 g L^{-1}, 30°C, 320 min, 30–100 mg L^{-1}	168.61	(Falaki and Bashiri, 2021)
Lignin copper ferrite	Synthetic solution	pH 8, 0.05 g, 27°C, 5 min, 50 mg L^{-1}	34.12	(Ali et al., 2022)
Apple stem	Synthetic solution	pH 10, 20 mg L^{-1}, 35°C, 20 min, 100 mg L^{-1}	153.85	(Takabi et al., 2021)
Chitosan-AC **	Real wastewater	pH 9, 10 g L^{-1}, 70°C, 25 min, 20–100 mg L^{-1}	12.50	(Kumari et al., 2017)
Chitosan-CS-NDIO **	Synthetic solution	pH 7.5, 7 mg, 35°C, 25 min., 20 mg L^{-1}	104.66	(Nasab et al., 2019)
Cyanobacteria, *Spirulina* sp.	Synthetic solution	pH 2, 500 g L^{-1}, 35°C, 180 min, 25–300 mg L^{-1}	101.87	(Guler et al., 2016)
Brown seaweed, *Sargassum wightii*	Synthetic solution	pH 7, 0.2 g, 30°C, 60 min, 80 mg L^{-1}	3.306	(Jayganesh et al., 2017)
Red seaweed, *Gracilaria corticata*	Synthetic solution	pH 8, 5 g, 25°C, 360 min, 100 mg L^{-1}	181.0	(Jegan et al., 2016)

(Continued)

TABLE 4 Continued

Adsorbent	Pollutant Type	Optimized Conditions *	q_{max} (mg g^{-1})	References
Red seaweed, *Kappaphycus alvarezii*	Synthetic solution	pH 8, 5 g, 25°C, 360 min, 100 mg L^{-1}	171.9	(Jegan et al., 2016)
Red seaweed *Gracilaria corticata*-AC ***	Synthetic solution	pH 5, 1 g, 30°C, 50 min, 80 mg L^{-1}	16.477	(Duraipandian et al., 2017)
Red seaweed, *Pterocladia capillacea*	Synthetic solution	pH 3, 0.4 g, 25°C, 60 min, 0.3 g L^{-1}	5.714	This work

*The optimized conditions ordering as the following: pH, adsorbent dose (g), temperature (°C), contact time (min or h), and CV dye concentration (mg L^{-1}). **Chitosan/nanodiopside nanocomposite (CS-NDIO), ***AC, Activited carbon.

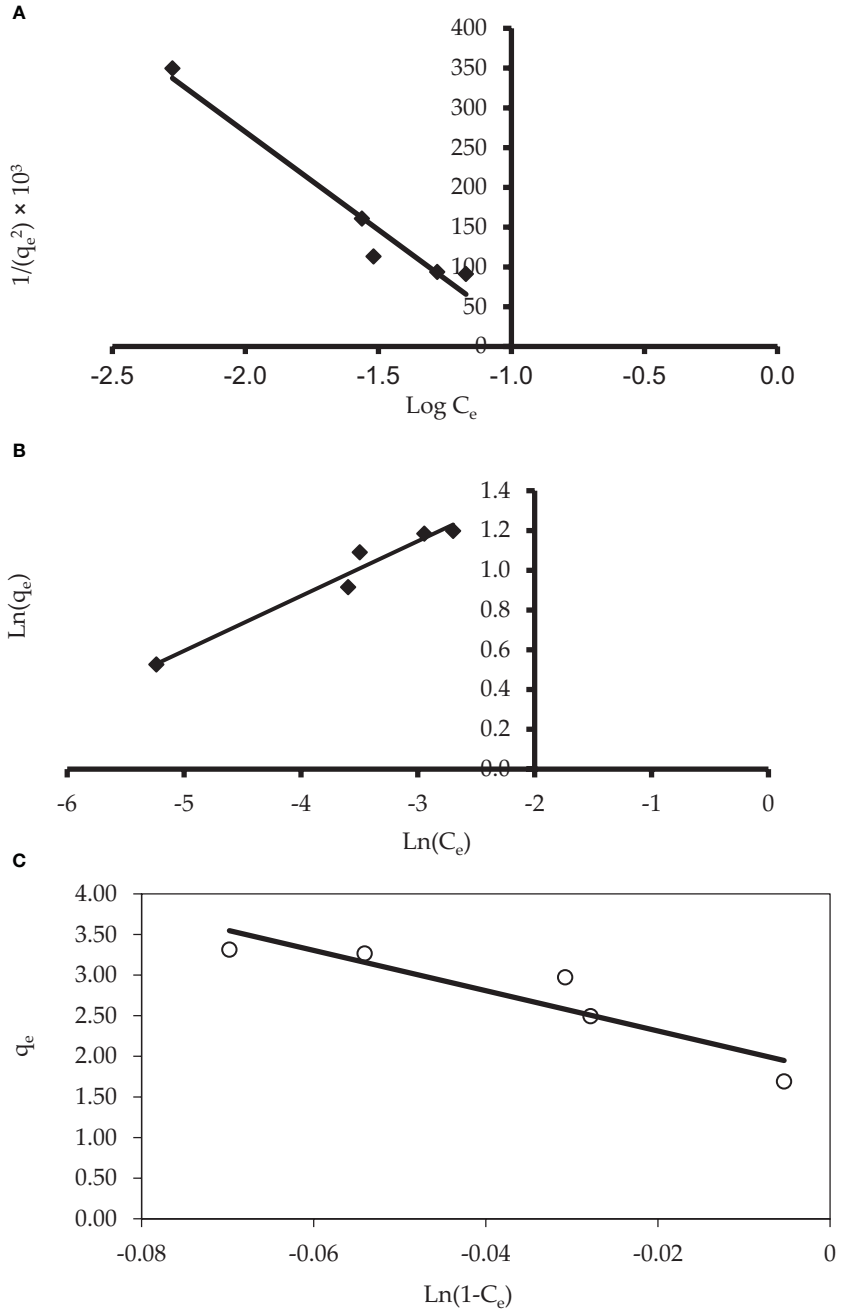

FIGURE 9
The fitting plot of Harkins–Jura **(A)**, Halsey **(B)**, and **(C)** Smith isotherm equations.

10.3389/fmars.2023.1202362

TABLE 5 The characteristics of real wastewater before and after treatment of CVD.

Parameters*	Before Treatment	After Treatment	Removal (%)
pH	7.62	7.07	7.21
Cond. (ms)	0.462	0.601	nd
Turb. (NTU)	77	11.81	84.66
TOC (mg L^{-1})	7784.0	nd	–
TSS (mg L^{-1})	2710	328	87.89
TDS (mg L^{-1})	2541	1011	60.21
Nitrate (mg L^{-1})	1.4	1.5	nd
Sulfate	2900	1819	37.27
Phosphate	5.7	2.2	61.40

*nd, Not detected; Cond,: Conductivity (ms); Turb, Turbidity (NTU); TOC, Total organic carbon (mg L–1); TSS, Total Suspended Solids (mg L–1); TDS, Total Dissolved Solid (mg L–1).

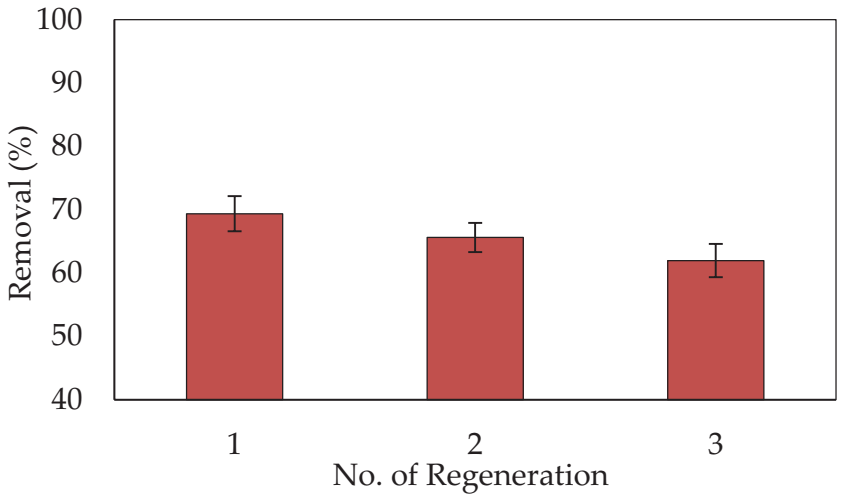

FIGURE 10
The regeneration cycles of *P. capillacea* and the removal percentages of CV dye (10 mg L^{-1} of CV at pH 3 and 25 °C, for 180 min on a shaker at 150 rpm).

3.7 Comparison with other adsorbents

Table 4 summarizes previous studies, as well as the present work, that uses a range of agricultural waste products to remove CV dye ions. According to the literature, many types of adsorbents have been investigated for their ability to remove CV dye. These adsorbent materials were widely available and less expensive than synthetic resins. These adsorbent materials include microalgae, seaweeds, extractives, hemicellulose, lignin, proteins, lipids, aqueous hydrocarbons, simple sugars, and starch, which include a variety of functional groups that help in ions complexation and dye sequestration (Shah et al., 2016). According to the data presented in Table 4, the studied agricultural natural adsorbents showed great effectiveness and selectivity for complexation with dye ions for the following reasons: (1) large numbers of hydroxyl and amino groups, (2) primary amino groups have a high degree of reactivity, and (3) polymer chains give suitable configurations. Because of the high adsorption capacity of the investigated adsorbents, it is a preferred and extremely appealing alternative adsorption material.

3.8 Quality of the treated wastewater and optimum conditions

To evaluate the impact of *P. capillacea* as an adsorbent, wastewater mixed well with simulated dye samples was collected to examine the removal of CV dye by the adsorbent under optimized conditions. Researchers should consider all characteristics of synthetic wastewater when designing an experiment that will employ it. The optimization parameters applied were 25°C, 0.4 g, pH 3, and 30 min contact time. The results confirmed that the highest removal was achieved for inorganic contaminants. The efficiency of the adsorption process increased for TSS, TDS, Sulphate, and Phosphate, with ranges of 2710-238 (mg L^{-1}), 1.254–1011 (mg L^{-1}), 2900-181 (mg L^{-1}), and 2.7–2.2 (mg L^{-1}),

respectively, with a percentage elimination of 87.89, 60.21, 37.27, and 61.40%, respectively. Meanwhile, Nitrate dropped from 2900 to 1819 mg L^{-1}. The wastewater effluents employed in this study contained significant concentrations of mixed effluents as pollutants from pond effluents from aquaculture, industrial, and textile processes, which competed with ammonia ions at the active sites and reduced removal efficiency. Several pollutants, including dyes and others of some which are not biodegradable, are present in textile effluent. Algae biomass can change several forms of inorganic nitrogen in wastewater into organic nitrogen. The primary mechanisms for nitrogen removal in algal systems have been demonstrated in prior research to be nitrification or denitrification, as well as biological nitrogen uptake by distributed biomass. A treated sample under these optimum operating conditions was used and is displayed in Table 5.

4 Conclusions

This study aims to remove different initial concentrations of toxic crystal Violet a textile dye, which pollutes the marine environment from aqueous solutions using red algae *P. capillacea.* The maximum sorption of CV dye onto *P. capillacea* was achieved at 25°C, 0.3 g, pH 3, for 30 min. With just 0.05 g of *P. capillacea*, a significant quantity of dye can be removed from wastewater in as little as 15 min (approximately 87.21% for synthetic wastewater). The average BET surface area (87.1721 m^2 g^{-1}) and total pore volume of 0.10368 cm^3 g^{-1} were obtained. FTIR analyses showed that functional groups such as carboxyl, carbonyl, and hydroxyl, amino have been found within a variety of biomolecules, proteins, and polysaccharides. Meanwhile the UV-visible absorption confirmed the presence of phenolic and alkaloid chemicals in the marine algal. The experimental results were analyzed using several isotherm equations, including Langmuir, Freundlich, Tempkin, Harkins–Jura, Halsey, and Smith models. From the Freundlich equation, the adsorption intensity (1/n) parameter had a small value of 0.959, including favorable adsorption. However, the kinetics of CV dye adsorption onto red alga followed the Pseudo-Second-Order model, which considers rates of ion exchange adsorption during the beginning of adsorption. Also, the thermodynamic parameters of ΔH° and ΔG° parameters showed exothermic as well as spontaneous adsorption processes. Additionally, for economic use, *P. capillacea* can be reused and it was found that the percentage removal decreased to 61.97% after three cycles of regeneration for synthetic wastewater. This mechanism entraps CV dye ions in materials with adsorptive features, such as active functional groups, highly porous structures, and large surface area, through physical or chemical interactions. Therefore, this study offer new insights into the effectiveness of the red algae *P. capillacea*, which may have great promise for crystal violet dye applications in wastewater treatment.

Data availability statement

The original contributions presented in the study are included in the article/Supplementary Material. Further inquiries can be directed to the corresponding author.

Author contributions

Conceptualization: AA and MA; methodology: AA and MA; software: AA and MA; validation: AA and MA; formal analysis: AA and MA; investigation: AA and MA; resources: SA-S, AA, and MA; data curation: AA, SA-S, and MA; writing—original draft preparation: AA, SA-S, and MA; writing—review and editing: AA, SA-S, and MA; visualization: AA, SA-S, and MA; supervision: AA; project administration: MA; funding acquisition: AA, SA-S, and MA. All authors contributed to the article and approved the submitted version.

Funding

Princess Nourah bint Abdulrahman University Researchers Supporting Project number (PNURSP2023R58), Princess Nourah bint Abdulrahman University, Riyadh, Saudi Arabia.

Acknowledgments

The authors express their gratitude to the support of Princess Nourah bint Abdulrahman University Researchers Supporting Project number (PNURSP2023R58), Princess Nourah bint Abdulrahman University, Riyadh, Saudi Arabia.

Conflict of interest

The authors declare that the research was conducted in the absence of any commercial or financial relationships that could be construed as a potential conflict of interest.

Publisher's note

Supplementary material

The Supplementary Material for this article can be found online at: https://www.frontiersin.org/articles/10.3389/fmars.2023.1202362/full#supplementary-material

References

Abate, G. Y., Alene, A. N., Habte, A. T., and Getahun, D. M. (2020). Adsorptive removal of malachite green dye from aqueous solution onto activated carbon of Catha edulis stem as a low cost bio-adsorbent. *Environ. Syst. Res.* 9, 1–13. doi: 10.1186/s40068-020-00191-4

Abdel Wahab, O. (2007). Kinetic and isotherm studies of copper (II) removal from wastewater using various adsorbents. *Egy. J. Aquat. Res.* 33, 125–143.

Abdi, O., and Kazemi, M. (2015). A review study of biosorption of heavy metals and comparison between different biosorbents. *J. Mater Environ. Sci.* 6, 1386–1399.

Abualnaja, K. M., Alprol, A. E., Abu-Saied, M. A., Ashour, M., and Mansour, A. T. (2021). Removing of anionic dye from aqueous solutions by adsorption using of multiwalled carbon nanotubes and poly (Acrylonitrile-styrene) impregnated with activated carbon. *Sustainability* 13, 7077. doi: 10.3390/su13137077

Ahluwalia, S. S., and Goyal, D. (2007). Microbial and plant derived biomass for removal of heavy metals from wastewater. *Bioresource Technol.* 98, 2243–2257. doi: 10.1016/j.biortech.2005.12.006

Ahmadi, S., Mohammadi, L., Rahdar, A., Rahdar, S., Dehghani, R., Adaobi Igwegbe, C., et al. (2020). Acid dye removal from aqueous solution by using neodymium (III) oxide nanoadsorbents. *Nanomaterials* 10, 556. doi: 10.3390/nano10030556

Akin, K., Ugraskan, V., Isik, B., and Cakar, F. (2022). Adsorptive removal of crystal violet from wastewater using sodium alginate-gelatin-montmorillonite ternary composite microbeads. *Int. J. Biol. Macromolecules*. 223, 543–554. doi: 10.1016/j.ijbiomac.2022.11.002

Aksu, Z. (2005). Application of biosorption for the removal of organic pollutants: a review. *Process Biochem.* 40, 997–1026. doi: 10.1016/j.procbio.2004.04.008

Alardhi, S. M., Alrubaye, J. M., and Albayati, T. M. (2020). Adsorption of Methyl Green dye onto MCM-41: equilibrium, kinetics and thermodynamic studies. *Desalination Water Treat* 179, 323–331. doi: 10.5004/dwt.2020.25000

Ali, R., Elsagan, Z., and Abdelhafez, S (2022). Lignin from Agro-Industrial Waste to an Efficient Magnetic Adsorbent for Hazardous Crystal Violet Removal. *Molecules*, 27, 1831

Al-Garni, S. M., Ghanem, K. M., Kabli, S. A., and Biag, A. K. (2013). Decolorization of crystal violet by mono and mixed bacterial culture techniques using optimized culture conditions. *Polish J. Environ. Stud.* 22.

Alprol, A. E. (2019). Study of environmental concerns of dyes and recent textile effluents treatment technology: A Review. *Asian J. Fisheries Aquat. Res.*, 1–18.

Alprol, A. E., Ashour, M., Mansour, A. T., Alzahrani, O. M., Mahmoud, S. F., and Gharib, S. M. (2021a). Assessment of water quality and phytoplankton structure of eight alexandria beaches, southeastern mediterranean sea, Egypt. *J. Mar. Sci. Eng.* 9, 1328. doi: 10.3390/jmse9121328

Alprol, A. E., El-Metwally, M., and Amer, A. (2019). *Sargassum latifolium* as eco-friendly materials for treatment of toxic nickel (II) and lead (II) ions from aqueous solution. *Egyptian J. Aquat. Biol. Fisheries* 23, 285–299. doi: 10.21608/ejabf.2019.66839

Alprol, A. E., Heneash, A. M. M., Ashour, M., Abualnaja, K. M., Alhashmialameer, D., Mansour, A. T., et al. (2021b). Potential Applications of *Arthrospira platensis* Lipid-Free Biomass in Bioremediation of Organic Dye from Industrial Textile Effluents and Its Influence on Marine Rotifer (*Brachionus plicatilis*). *Materials (Basel)* 14. doi: 10.3390/ma14164446

Alprol, A. E., Mansour, A. T., Abdelwahab, A. M., and Ashour, M. (2023a). Advances in green synthesis of metal oxide nanoparticles by marine algae for wastewater treatment by adsorption and photocatalysis techniques. *Catalysts* 13, 888. doi: 10.3390/catal13050888

Alprol, A. E., Mansour, A. T., El-Beltagi, H. S., and Ashour, M. (2023b). Algal extracts for green synthesis of zinc oxide nanoparticles: Promising approach for algae bioremediation. *Materials* 16, 2819. doi: 10.3390/ma16072819

Amer, A., and Abdel-Moneim, M. (2017). Bioremediation of Reactive Blue 19 and Reactive Black 5 from Aqueous Solution by using Fungi Aspergillus niger. *Int. J. Curr. Microbiol. App. Sci.* 6, 1676–1686. doi: 10.20546/ijcmas.2017.603.193

Anand, M., and Suresh, S. (2015). Marine seaweed *Sargassum wightii* extract as a low-cost sensitizer for ZnO photoanode based dye-sensitized solar cell. *Adv. Natural Sciences: Nanoscience Nanotechnology* 6, 035008.

Apha, (1926). *Standard methods for the examination of water and wastewater (American Public Health Association)* (Washington, D.C., USA: American Public Health Association).

Ashour, M., Alprol, A. E., Heneash, A. M. M., Saleh, H., Abualnaja, K. M., Alhashmialameer, D., et al. (2021). Ammonia bioremediation from aquaculture wastewater effluents using a*rthrospira platensis* NIOF17/003: Impact of biodiesel residue and potential of ammonia-loaded biomass as rotifer feed. *Materials (Basel)* 14, 5460. doi: 10.3390/ma14185460

Azizi, S., Mahdavi Shahri, M., and Mohamad, R. (2017). Green synthesis of zinc oxide nanoparticles for enhanced adsorption of lead ions from aqueous solutions: equilibrium, kinetic and thermodynamic studies. *Molecules* 22, 831. doi: 10.3390/molecules22060831

Babarinde, N. A., Oyesiku, O., and Dairo, O. F. (2007). Isotherm and thermodynamic studies of the biosorption of copper (II) ions by Erythrodontium barteri. *Int. J. Phys. Sci.* 2, 300–304.

Balabanova, M., Popova, L., and Tchipeva, R. (2004). Dyes in dermatology (Reprinted from J Dis Mon, vol 50, pg 270-9, 2004). *DM DISEASE-A-MONTH* 50, 270–279. doi: 10.1016/j.disamonth.2004.05.002

Banat, I. M., Nigam, P., Singh, D., and Marchant, R. (1996). Microbial decolorization of textile-dyecontaining effluents: a review. *Bioresource Technol.* 58, 217–227. doi: 10.1016/S0960-8524(96)00113-7

Bhatnagar, A., Jain, A., and Mukul, M. (2005). Removal of congo red dye from water using carbon slurry waste. *Environ. Chem. Lett.* 2, 199–202. doi: 10.1007/s10311-004-0097-0

Bhatti, H. N., Sadaf, S., Naz, M., Iqbal, M., Safa, Y., Ain, H., et al. (2021). Enhanced adsorption of Foron Black RD 3GRN dye onto sugarcane bagasse biomass and Na-alginate composite. *Desalination Water Treat* 216, 423–435. doi: 10.5004/dwt.2021.26893

Brinza, L., Dring, M. J., and Gavrilescu, M. (2007). Marine micro and macro algal species as biosorbents for heavy metals. *Environ. Eng. Manage. J. (EEMJ)* 6. doi: 10.30638/eemj.2007.029

Çelekli, A., İlgün, G., and Bozkurt, H. (2012). Sorption equilibrium, kinetic, thermodynamic, and desorption studies of Reactive Red 120 on Chara contraria. *Chem. Eng. J.* 191, 228–235. doi: 10.1016/j.cej.2012.03.007

Celekli, A., Yavuzatmaca, M., and Bozkurt, H. (2010). An eco-friendly process: predictive modelling of copper adsorption from aqueous solution on *Spirulina platensis*. *J. hazardous materials* 173, 123–129. doi: 10.1016/j.jhazmat.2009.08.057

Chen, K.-C., Wu, J.-Y., Liou, D.-J., and Hwang, S.-C. J. (2003). Decolorization of the textile dyes by newly isolated bacterial strains. *J. Biotechnol.* 101, 57–68. doi: 10.1016/S0168-1656(02)00303-6

Cheraghi, M., Sobhanardakani, S., Lorestani, B., and Zandipak, R. (2016). Tea wastes efficiency on removal of cd (ii) from aqueous solutions. *Arch. Hygiene Sci.* 5, 184–191.

Cheung, W., Szeto, Y., and Mckay, G. (2007). Intraparticle diffusion processes during acid dye adsorption onto chitosan. *Bioresource Technol.* 98, 2897–2904. doi: 10.1016/j.biortech.2006.09.045

Cusioli, L. F., Quesada, H. B., Baptista, A. T., Gomes, R. G., and Bergamasco, R. (2020). Soybean hulls as a low-cost biosorbent for removal of methylene blue contaminant. *Environ. Prog. Sustain. Energy* 39, e13328. doi: 10.1002/ep.13328

Dahri, M. K., Kooh, M. R. R., and Lim, L. B. (2014). Water remediation using low cost adsorbent walnut shell for removal of malachite green: equilibrium, kinetics, thermodynamic and regeneration studies. *J. Environ. Chem. Eng.* 2, 1434–1444. doi: 10.1016/j.jece.2014.07.008

Daneshvar, N., Khataee, A., Rasoulifard, M., and Pourhassan, M. (2007). Biodegradation of dye solution containing Malachite Green: Optimization of effective parameters using Taguchi method. *J. Hazardous Materials* 143, 214–219. doi: 10.1016/j.jhazmat.2006.09.016

Dawood, S. A. (2013). *Development and characterization of biomass based novel adsorbent in the removal of Congo red dye by adsorption* (Australia: Curtin University).

Dawood, S., and Sen, T. (2014). Review on dye removal from its aqueous solution into alternative cost effective and non-conventional adsorbents. *J. Chem. Process Eng.* 1, 1–11.

Diquarternasi, Y. (2009). Removal of basic blue 3 and reactive orange 16 by adsorption onto quartenized sugar cane bagasse. *Malaysian J. Analytical Sci.* 13, 185–193.

Docampo, R., and Moreno, S. N. (1990). The metabolism and mode of action of gentian violet. *Drug Metab. Rev.* 22, 161–178. doi: 10.3109/03602539009041083

Duraipandian, J., Rengasamy, T., and Vadivelu, S. (2017). Experimental and modeling studies for the removal of crystal violet dye from aqueous solutions using eco-friendly Gracilaria corticata seaweed activated carbon/Zn/Alginate Polymeric composite beads. *Journal of polymers and the environment*, 25, 1062–1071.

El-Agawany, N. I., Abdel-Razik, S. A., Abdel-Kareem, M. S., and Kaamoush, M. I. (2023). Environmental performance of two marine algae Ulva fasciata and Pterocladia capillacea in the biological treatment of four reactive dyes from aqueous solutions based on fresh and dried biomass. *Appl. Water Sci.* 13, 82. doi: 10.1007/s13201-023-01893-7

El-Din, S. M. M., Noaman, N. H., and Zaky, S. H. (2016). Effects of chloramphenicol, clofibric acid, acetyl salicylic acid, nonylphenol and bisphenol on the protein profile and ultrastructure of marine macroalgae Pterocladia capillacea and Ulva lactuca. *Egypt J. Bot.* 56, 335–352. doi: 10.21608/ejbo.2016.392

El Nemr, A., El-Sikaily, A., Khaled, A., and Abdelwahab, O. (2015). Removal of toxic chromium from aqueous solution, wastewater and saline water by marine red alga Pterocladia capillacea and its activated carbon. *Arabian J. Chem.* 8, 105–117. doi: 10.1016/j.arabjc.2011.01.016

El-Said, G. F., El-Sadaawy, M. M., and Aly-Eldeen, M. A. (2018). Adsorption isotherms and kinetic studies for the defluoridation from aqueous solution using eco-friendly raw marine green algae, Ulva lactuca. *Environ. Monit. Assess.* 190, 1–15. doi: 10.1007/s10661-017-6392-6

El-Shouny, W., Sharaf, M., Abomohra, A., and Abo-Eleneen, M. (2015). Production enhancement of some valuable compounds of *Arthrospira Platensis*. *J. Basic Environ. Sci.* 2, 74–83.

El-Sikaily, A., El Nemr, A., and Khaled, A. (2011). Copper sorption onto dried red alga *Pterocladia capillacea* and its activated carbon. *Chem. Eng. J.* 168, 707–714. doi: 10.1016/j.cej.2011.01.064

Erdogan, Y., Isik, B., Ugraskan, V., and Cakar, F. (2022). Effective and fast removal of crystal violet dye from aqueous solutions using Rumex acetosella: isotherm, kinetic, thermodynamic studies, and statistical analysis. *Biomass Conversion Biorefinery*, 1–16. doi: 10.1007/s13399-022-02349-9

Ergene, A., Ada, K., Tan, S., and Katırcıoğlu, H. (2009). Removal of Remazol Brilliant Blue R dye from aqueous solutions by adsorption onto immobilized Scenedesmus quadricauda: Equilibrium and kinetic modeling studies. *Desalination* 249, 1308–1314. doi: 10.1016/j.desal.2009.06.027

Falaki, Z., and Bashiri, H. (2021). Preparing an adsorbent from the unused solid waste of Rosewater extraction for high efficient removal of Crystal Violet. *Journal of the Iranian Chemical Society*, 18, 2689–2702.

Foo, K. Y., and Hameed, B. H. (2010). Insights into the modeling of adsorption isotherm systems. *Chem. Eng. J.* 156, 2–10. doi: 10.1016/j.cej.2009.09.013

Foo, K., and Hameed, B. (2011). Microwave assisted preparation of activated carbon from pomelo skin for the removal of anionic and cationic dyes. *Chem. Eng. J.* 173, 385–390. doi: 10.1016/j.cej.2011.07.073

Freundlich, H. (1906). *Über die Adsorption in Lösungen*. (Leipzig, Germany: Wilhelm Engelmann).

Ghaedi, M., Biyareh, M. N., Kokhdan, S. N., Shamsaldini, S., Sahraei, R., Daneshfar, A., et al. (2012). Comparison of the efficiency of palladium and silver nanoparticles loaded on activated carbon and zinc oxide nanorods loaded on activated carbon as new adsorbents for removal of Congo red from aqueous solution: Kinetic and isotherm study. *Materials Sci. Engineering: C* 32, 725–734. doi: 10.1016/j.msec.2012.01.015

Ghoneim, M. M., El-Desoky, H. S., El-Moselhy, K. M., Amer, A., Abou El-Naga, E. H., Mohamedein, L. I., et al. (2014). Removal of cadmium from aqueous solution using marine green algae, *Ulva lactuca*. *Egyptian J. Aquat. Res.* 40, 235–242. doi: 10.1016/j.ejar.2014.08.005

Halsey, G. D. (1952). *The role of surface heterogeneity in adsorption. Advances in catalysis* (Elsevier).

Guler, U. A., Ersan, M., Tuncel, E., and Dügenci, F. (2016). Mono and simultaneous removal of crystal violet and safranin dyes from aqueous solutions by HDTMA-modified Spirulina sp. *Process Safety and Environmental Protection*, 99, 194–206.

Harkins, W. D., and Jura, G. (1944). Surfaces of solids. XIII. A vapor adsorption method for the determination of the area of a solid without the assumption of a molecular area, and the areas occupied by nitrogen and other molecules on the surface of a solid. *J. Am. Chem. Soc.* 66, 1366–1373. doi: 10.1021/ja01236a048

Ho, Y.-S., and Mckay, G. (1999). Pseudo-second order model for sorption processes. *Process Biochem.* 34, 451–465. doi: 10.1016/S0032-9592(98)00112-5

Isik, B., Avci, S., Cakar, F., and Cankurtaran, O. (2022). Adsorptive removal of hazardous dye (crystal violet) using bay leaves (Laurus nobilis L.): surface characterization, batch adsorption studies, and statistical analysis. *Environ. Sci. pollut. Res.*, 1–24.

Jayganesh, D., Tamilarasan, R., Kumar, M., Murugavelu, M., and Sivakumar, V. (2017). Equilibrium and Modelling Studies for the Removal of Crystal Violet Dye from aqueous solution using eco-friendly activated carbon prepared from Sargassm wightii seaweeds. *J Mater Environ Sci*, 8, 1508–1517.

Jegan, J., Vijayaraghavan, J., Bhagavathi Pushpa, T., and Sardhar Basha, S. (2016). Application of seaweeds for the removal of cationic dye from aqueous solution. *Desalination and Water Treatment*, 57, 25812–25821.

Kareem, A., Abd Alrazak, N., Aljebori, K. H., Aljebori, A., Algboory, H. L., and Alkaim, A. F. (2016). Removal of methylene blue dye from aqueous solutions by using activated carbon/ureaformaldehyde composite resin as an adsorbent. *Int. J. Chem. Sci.* 14, 635–648.

Khattri, S., and Singh, M. (2000). Colour removal from synthetic dye wastewater using a bioadsorbent. *Water Air Soil pollut.* 120, 283–294. doi: 10.1023/A:1005207803041

Kokabi, M., Yousefzadi, M., Nejad Ebrahimi, S., and Zarei, M. (2017). Green synthesis of zinc oxide nanoparticles using Seaweed aqueous extract and evaluation of antibacterial and ecotoxicological activity. *J. @ Persian Gulf (Marine Science)* 8, 61–72. doi: 10.29252/jpg.8.27.61

Kooh, M. R. R., Dahri, M. K., and Lim, L. B. (2016). The removal of rhodamine B dye from aqueous solution using Casuarina equisetifolia needles as adsorbent. *Cogent Environ. Sci.* 2, 1140553. doi: 10.1080/23311843.2016.1140553

Kumari, H. J., Krishnamoorthy, P., Arumugam, T., Radhakrishnan, S., and Vasudevan, D. (2017). An efficient removal of crystal violet dye from waste water by adsorption onto TLAC/Chitosan composite: a novel low cost adsorbent. *International journal of biological macromolecules*, 96, 324–333.

Kusvuran, E., Gulnaz, O., Samil, A., and Yildirim, Ö. (2011). Decolorization of malachite green, decolorization kinetics and stoichiometry of ozone-malachite green and removal of antibacterial activity with ozonation processes. *J. hazardous materials* 186, 133–143. doi: 10.1016/j.jhazmat.2010.10.100

Lagergren, S. K. (1898). About the theory of so-called adsorption of soluble substances. *Sven. Vetenskapsakad. Handingarl* 24, 1–39.

Langmuir, I. (1916). The constitution and fundamental properties of solids and liquids. Part I. Solids. *J. Am. Chem. Soc.* 38, 2221–2295. doi: 10.1021/ja02268a002

Lee, C., Low, K., and Gan, P. (1999). Removal of some organic dyes by acid-treated spent bleaching earth. *Environ. Technol.* 20, 99–104. doi: 10.1080/09593332008616798

Lee, S.-L., Park, J.-H., Kim, S.-H., Kang, S.-W., Cho, J.-S., Jeon, J.-R., et al. (2019). Sorption behavior of malachite green onto pristine lignin to evaluate the possibility as a dye adsorbent by lignin. *Appl. Biol. Chem.* 62, 1–10. doi: 10.1186/s13765-019-0444-2

Liang, S., Guo, X., Feng, N., and Tian, Q. (2010). Isotherms, kinetics and thermodynamic studies of adsorption of Cu2+ from aqueous solutions by Mg2+/K+ type orange peel adsorbents. *J. hazardous materials* 174, 756–762. doi: 10.1016/j.jhazmat.2009.09.116

Littlefield, N. A., Blackwell, B.-N., Hewitt, C. C., and Gaylor, D. W. (1985). Chronic toxicity and carcinogenicity studies of gentian violet in mice. *Toxicological Sci.* 5, 902–912. doi: 10.1093/toxsci/5.5.902

Lorenc-Grabowska, E., and Gryglewicz, G. (2007). Adsorption characteristics of Congo Red on coal-based mesoporous activated carbon. *Dyes pigments* 74, 34–40. doi: 10.1016/j.dyepig.2006.01.027

Machado, F. M., Bergmann, C. P., Lima, E. C., Adebayo, M. A., and Fagan, S. B. (2014). Adsorption of a textile dye from aqueous solutions by carbon nanotubes. *Materials Res.* 17, 153–160. doi: 10.1590/S1516-14392013005000204

Mansour, A. T., Alprol, A. E., Abualnaja, K. M., El-Beltagi, H. S., Ramadan, K. M. A., and Ashour, M. (2022a). Dried brown seaweed's phytoremediation potential for methylene blue dye removal from aquatic environments. *Polymers* 14. doi: 10.3390/polym14071375

Mansour, A. T., Alprol, A. E., Abualnaja, K. M., El-Beltagi, H. S., Ramadan, K. M. A., and Ashour, M. (2022b). The using of nanoparticles of microalgae in remediation of toxic dye from industrial wastewater: Kinetic and isotherm studies. *Materials (Basel)* 15. doi: 10.3390/ma15113922

Mansour, A. T., Alprol, A. E., Ashour, M., Ramadan, K. M., Alhajji, A. H., and Abualnaja, K. M. (2022c). Do red seaweed nanoparticles enhance bioremediation capacity of toxic dyes from aqueous solution? *Gels* 8, 310. doi: 10.3390/gels8050310

Mansour, A. T., Alprol, A. E., Khedawy, M., Abualnaja, K. M., Shalaby, T. A., Rayan, G., et al. (2022d). Green synthesis of zinc oxide nanoparticles using red seaweed for the elimination of organic toxic dye from an aqueous solution. *Materials* 15, 5169. doi: 10.3390/ma15155169

Mansour, A. T., Ashour, M., Alprol, A. E., and Alsaqufi, A. S. (2022e). Aquatic plants and aquatic animals in the context of sustainability: Cultivation techniques, integration, and blue revolution. *Sustainability* 14, 3257. doi: 10.3390/su14063257

Mashkoor, F., and Nasar, A. (2020). Magsorbents: Potential candidates in wastewater treatment technology–A review on the removal of methylene blue dye. *J. magnetism magnetic materials* 500, 166408. doi: 10.1016/j.jmmm.2020.166408

Mbacké, M. K., Kane, C., Diallo, N. O., Diop, C. M., Chauvet, F., Comtat, M., et al. (2016). Electrocoagulation process applied on pollutants treatment-experimental optimization and fundamental investigation of the crystal violet dye removal. *J. Environ. Chem. Eng.* 4, 4001–4011. doi: 10.1016/j.jece.2016.09.002

Meena, A. K., Mishra, G., Rai, P., Rajagopal, C., and Nagar, P. (2005). Removal of heavy metal ions from aqueous solutions using carbon aerogel as an adsorbent. *J. hazardous materials* 122, 161–170. doi: 10.1016/j.jhazmat.2005.03.024

Miller, J. A., and Miller, E. C. (1953). *The carcinogenic aminoazo dyes. Advances in cancer research* (Elsevier).

Nasab, S. G., Semnani, A., Teimouri, A., Yazd, M. J., Isfahani, T. M., and Habibollahi, S. (2019). Decolorization of crystal violet from aqueous solutions by a novel adsorbent chitosan/nanodiopside using response surface methodology and artificial neural network-genetic algorithm. *International journal of biological macromolecules*, 124, 429–443.

Nassar, N. N., Marei, N. N., Vitale, G., and Arar, L. A. (2015). Adsorptive removal of dyes from synthetic and real textile wastewater using magnetic iron oxide nanoparticles: thermodynamic and mechanistic insights. *Can. J. Chem. Eng.* 93, 1965–1974. doi: 10.1002/cjce.22315

Ng, J., Cheung, W., and Mckay, G. (2002). Equilibrium studies of the sorption of Cu (II) ions onto chitosan. *J. colloid Interface Sci.* 255, 64–74. doi: 10.1006/jcis.2002.8664

Özacar, M., and Şengil, İ.A. (2004). Application of kinetic models to the sorption of disperse dyes onto alunite. *Colloids Surfaces A: Physicochemical Eng. aspects* 242, 105–113. doi: 10.1016/j.colsurfa.2004.03.029

Padilha, F. P., De França, F. P., and Da Costa, A. C. A. (2005). The use of waste biomass of Sargassum sp. for the biosorption of copper from simulated semiconductor effluents. *Bioresource Technol.* 96, 1511–1517. doi: 10.1016/j.biortech.2004.11.009

Pathania, D., Sharma, S., and Singh, P. (2017). Removal of methylene blue by adsorption onto activated carbon developed from Ficus carica bast. *Arabian J. Chem.* 10, S1445–S1451. doi: 10.1016/j.arabjc.2013.04.021

Potgieter, J., Pearson, S., and Pardesi, C. (2018). Kinetic and thermodynamic parameters for the adsorption of methylene blue using fly ash under batch, column, and heap leaching configurations. *Coal combustion gasification products* 10, 23–33.

Putri, K. N.A., Keereerak, A., and Chinpa, W. (2020). Novel cellulose-based biosorbent from lemongrass leaf combined with cellulose acetate for adsorption of crystal violet. *International Journal of Biological Macromolecules*, 156, 762–772.

Rajeswari, R., and Jeyaprakash, K. (2019). Bioactive potential analysis of brown seaweed Sargassum wightii using UV-VIS and FT-IR. *J. Drug Delivery Ther.* 9, 150–153. doi: 10.22270/jddt.v9i1.2199

Sahu, N., and Saxena, J. (2013). Phytochemical analysis of Bougainvillea glabra Choisy by FTIR and UV-VIS spectroscopic analysis. *Int. J. Pharm. Sci. Rev. Res.* 21, 196–198.

Salleh, M. A. M., Mahmoud, D. K., Karim, W. A. W. A., and Idris, A. (2011). Cationic and anionic dye adsorption by agricultural solid wastes: a comprehensive review. *Desalination* 280, 1–13. doi: 10.1016/j.desal.2011.07.019

Sarabadan, M., Bashiri, H., and Mousavi, S. M. (2019). Removal of crystal violet dye by an efficient and low cost adsorbent: modeling, kinetic, equilibrium and thermodynamic studies. *Korean Journal of Chemical Engineering*, 36, 1575–1586.

Sarı, A., and Tuzen, M. (2009). Kinetic and equilibrium studies of biosorption of Pb (II) and Cd (II) from aqueous solution by macrofungus (Amanita rubescens) biomass. *J. hazardous materials* 164, 1004–1011. doi: 10.1016/j.jhazmat.2008.09.002

Shah, J., Kumar, S., Sharma, S., Sharma, R., and Sharma, R. (2016). Removal of nickel from aqueous solution by using low cost adsorbents: a review. *Int. J. Sci. Eng. Appl. Sci.* 2, 2395–3470.

Shao, W., Ebaid, R., El-Sheekh, M., Abomohra, A., and Eladel, H. (2019). Pharmaceutical applications and consequent environmental impacts of *Spirulina* (*Arthrospira*): An overview. *Grasas y Aceites* 70, e292–e292. doi: 10.3989/gya.0690181

Sharma, S., Saxena, R., and Gaur, G. (2014). Study of removal techniques for azo dyes by biosorption: a review. *IOSR J. Appl. Chem.* 7. doi: 10.9790/5736-071010621

Singh, S., Anil, A. G., Khasnabis, S., Kumar, V., Nath, B., Adiga, V., et al. (2022). Sustainable removal of Cr (VI) using graphene oxide-zinc oxide nanohybrid: Adsorption kinetics, isotherms and thermodynamics. *Environ. Res.* 203, 111891. doi: 10.1016/j.envres.2021.111891

Smith, S. E. (1947). The sorption of water vapor by high polymers. *J. Am. Chem. Soc.* 69, 646–651. doi: 10.1021/ja01195a053

Srinivasan, A., and Viraraghavan, T. (2010). Decolorization of dye wastewaters by biosorbents: a review. *J. Environ. Manage.* 91, 1915–1929. doi: 10.1016/j.jenvman.2010.05.003

Sulyman, M. (2014). "Fixed-bed column packed with low-cost spent tea leaves for the removal of crystal violet from aqueous solution," in *5th International Conference on Environmental Science and Technology*, Gdansk-Poland.

Surchi, K. M. S. (2011). Agricultural wastes as low cost adsorbents for Pb removal: kinetics, equilibrium and thermodynamics. *Int. J. Chem.* 3, 103. doi: 10.5539/ijc.v3n3p103

Takabi, A. S., Shirani, M., and Semnani, A. (2021). Apple stem as a high performance cellulose based biosorbent for low cost and eco-friendly adsorption of crystal violet from aqueous solutions using experimental design: Mechanism, kinetic and thermodynamics. *Environmental Technology & Innovation*, 24, 101947

Tahir, M. A., Bhatti, H. N., and Iqbal, M. (2016). Solar Red and Brittle Blue direct dyes adsorption onto Eucalyptus angophoroides bark: Equilibrium, kinetics and thermodynamic studies. *J. Environ. Chem. Eng.* 4, 2431–2439. doi: 10.1016/j.jece.2016.04.020

Temkin, M. (1940). Kinetics of ammonia synthesis on promoted iron catalysts. *Acta physiochim. URSS* 12, 327–356.

Uyar, T., Havelund, R., Hacaloglu, J., Besenbacher, F., and Kingshott, P. (2010). Functional electrospun polystyrene nanofibers incorporating α-, β-, and γ-cyclodextrins: comparison of molecular filter performance. *ACS nano* 4, 5121–5130. doi: 10.1021/nn100954z

Villaescusa, I., Fiol, N., MartúNez, M. a., Miralles, N., Poch, J., and Serarols, J. (2004). Removal of copper and nickel ions from aqueous solutions by grape stalks wastes. *Water Res.* 38, 992–1002. doi: 10.1016/j.watres.2003.10.040

Weber, J. W.J., and Morris, J. C. (1963). Kinetics of adsorption on carbon from solution. *J. sanitary Eng. division* 89, 31–59. doi: 10.1061/JSEDAI.0000430

Yan, Y., Xiang, B., Li, Y., and Jia, Q. (2013). Preparation and adsorption properties of diethylenetriamine-modified chitosan beads for acid dyes. *J. Appl. Polymer Sci.* 130, 4090–4098. doi: 10.1002/app.39691

Yeamin, M. B., Islam, M. M., Chowdhury, A.-N., and Awual, M. R. (2021). Efficient encapsulation of toxic dyes from wastewater using several biodegradable natural polymers and their composites. *J. Cleaner Production* 291, 125920. doi: 10.1016/j.jclepro.2021.125920